NEUROSYSTEMS

Information processing from the motor cortices to the subthalamic nucleus and globus pallidus and their somatotopic organizations revealed electrophysiologically in monkeys

Hirokazu Iwamuro,[1,2,3] (iD) Yoshihisa Tachibana,[1,4] (iD) Yoshikazu Ugawa,[5] (iD) Nobuhito Saito[2] and Atsushi Nambu[1] (iD)

[1]Division of System Neurophysiology, National Institute for Physiological Sciences and Department of Physiological Sciences, SOKENDAI (Graduate University for Advanced Studies), 38 Nishigonaka, Myodaiji, Okazaki, Aichi 444-8585, Japan
[2]Department of Neurosurgery, Graduate School of Medicine, The University of Tokyo, Tokyo, Japan
[3]Department of Research and Therapeutics for Movement Disorders, Juntendo University Graduate School of Medicine, Tokyo, Japan
[4]Division of System Neuroscience, Kobe University Graduate School of Medicine, Kobe, Japan
[5]Department of Neurology, School of Medicine, Fukushima Medical University and Fukushima Global Medical Science Center, Advanced Clinical Research Center, Fukushima Medical University, Fukushima, Japan

Abstract

To understand how the information derived from different motor cortical areas representing different body parts is organized in the basal ganglia, we examined the neuronal responses in the subthalamic nucleus (STN), and the external (GPe) and internal (GPi) segments of the globus pallidus (input, relay and output nuclei, respectively) to stimulation of the orofacial, forelimb and hindlimb regions of the primary motor cortex (MI) and supplementary motor area (SMA) in macaque monkeys under the awake state. Most STN and GPe/GPi neurons responded exclusively to stimulation of either the MI or SMA, and one-fourth to one-third of neurons responded to both. STN neurons responding to the hindlimb, forelimb and orofacial regions of the MI were located along the medial–lateral axis in the posterolateral STN, while neurons responding to the orofacial region of the SMA were located more medially than the others in the anteromedial STN. GPe/GPi neurons responding to the hindlimb, forelimb and orofacial regions of the MI were found along the dorsal–ventral axis in the posterolateral GPe/GPi, and neurons responding to the corresponding regions of the SMA were similarly but less clearly distributed in more anteromedial regions. Moreover, neurons responding to the distal and proximal forelimb MI regions were found along the lateral–medial axis in the STN and the ventral–dorsal axis in the GPe/GPi. Most STN and GPe/GPi neurons showed kinaesthetic responses with similar somatotopic maps. These observations suggest that the somatotopically organized inputs from the MI and SMA are well preserved in the STN and GPe/GPi with partial convergence.

Introduction

To elucidate the functions of the basal ganglia in normal and disease states, it is essential to understand how information derived from the cerebral cortex is processed through the cortico-basal ganglia loop (Alexander *et al.*, 1986; Alexander & Crutcher, 1990a). The striatum and subthalamic nucleus (STN) are the input stations of the basal ganglia and receive excitatory cortical inputs. On the other hand, the internal segment of the globus pallidus (GPi) and the substantia nigra pars reticulata (SNr) are the output nuclei of the basal ganglia. Information from the cerebral cortex reaches the output nuclei via the following three major pathways: the cortico-STN-GPi/SNr hyperdirect, cortico-striato-GPi/SNr direct and cortico-striato-external pallido (GPe)-STN-GPi/SNr indirect pathways (Albin *et al.*, 1989; Alexander & Crutcher, 1990a; Nambu *et al.*, 2002a).

One of the key concepts of basal ganglia circuitry is the parallel processing hypothesis vs. the information convergence hypothesis. The parallel processing hypothesis proposes that information

derived from different cortical areas is processed in parallel through different cortico-basal ganglia loops (Alexander *et al.*, 1986; Hoover & Strick, 1993; Strick *et al.*, 1995). The information convergence hypothesis proposes that inputs derived from different cortical areas are converged and integrated into the cortico-basal ganglia loops (Percheron & Filion, 1991; Percheron *et al.*, 1994). Among them, the motor loop that originates from the primary motor cortex (MI), supplementary motor area (SMA) and premotor cortex (PM) has been most extensively analysed (Nambu *et al.*, 1996; Takada *et al.*, 1998; Nambu, 2011), and how information from different cortical areas is transferred to the basal ganglia has long been a focus of attention. Recent studies have suggested that parallel processing and information convergence may both occur within the basal ganglia (Haber *et al.*, 2006; Nambu, 2011; Haynes & Haber, 2013). In fact, in the striatum, projections from the MI, SMA and PM overlap partially (Takada *et al.*, 1998), and one-fourth of striatal neurons receive convergent inputs from both the MI and SMA (Nambu *et al.*, 2002b). On the other hand, in the STN, axon terminals from the MI and SMA are partially intermingled (Nambu *et al.*, 1996), but whether these projections converge at a single neuron level remains to be determined. Additionally, how information from different motor cortical areas is organized in the GPe and GPi remains to be clarified. The first objective of this study is to electrophysiologically investigate how MI- and SMA-inputs are represented at a single neuron level in the STN and GPe/GPi through the cortico-basal ganglia pathway.

Another key concept of basal ganglia circuitry is somatotopic organization. Somatotopy in the striatum has been confirmed by both anatomical and electrophysiological studies (Künzle, 1975; Alexander & DeLong, 1985; Alexander & Crutcher, 1990b; Flaherty & Graybiel, 1993; Takada *et al.*, 1998; Nambu *et al.*, 2002b; Takara *et al.*, 2011). Somatotopy in the STN has also been revealed by anatomical and electrophysiological studies (Monakow *et al.*, 1978; DeLong *et al.*, 1985; Wichmann *et al.*, 1994; Nambu *et al.*, 1996). However, STN neurons have wide dendritic fields that cover large areas of the STN (Yelnik & Percheron, 1979), and their local axon collaterals terminate on neighbouring neurons in rodents (Kita *et al.*, 1983), although they are not identified in primates (Sato *et al.*, 2000). Therefore, somatotopic organization at a single neuron level is still not clear in the STN. On the other hand, somatotopy in the posterior parts of the GPe/GPi that mainly processes MI-inputs has been demonstrated electrophysiologically (DeLong, 1971; Georgopoulos *et al.*, 1983; DeLong *et al.*, 1985; Hamada *et al.*, 1990; Nambu *et al.*, 1990; Yoshida *et al.*, 1993), but the more anterior and medial parts that are thought to process SMA-inputs have not been well studied yet. The second objective of this study is to elucidate somatotopic maps in the STN and GPe/GPi at a single neuron level by electrophysiologically analysing cortical inputs from the MI and SMA at the same time. The importance of somatotopic maps in the STN and GPi should be emphasized given the fact that they are clinically utilized to localize the target areas for stereotactic surgery for the treatment of movement disorders, including Parkinson's disease, dyskinesia and dystonia (Vitek *et al.*, 1999; Gross *et al.*, 2006; Obeso *et al.*, 2008; Maiti *et al.*, 2016).

Here, we performed recordings of neuronal activity in the STN and GPe/GPi of the monkey, and extensively investigated their responses to stimulation of the orofacial, forelimb and hindlimb regions of the MI and SMA to clarify information processing and somatotopic maps in the STN and GPe/GPi.

Materials and methods

Animals

Two adult female monkeys (*P8*, *Macaca fuscata* and *P6*, *Macaca cyclopis*; body weight 4.0–5.0 kg) were used in this study. They were trained daily to quietly sit in a monkey chair. *Monkey P8* was trained to be accustomed to passive movements of body parts. The experimental protocols were approved by the Institutional Animal Care and Use Committee of National Institutes of Natural Sciences. All experiments were conducted according to the guidelines of the National Institutes of Health *Guide for the Care and Use of Laboratory Animals*.

Surgery and MRI acquisition

Under general anaesthesia with ketamine hydrochloride (10 mg/kg body weight, i.m.), xylazine hydrochloride (1 mg/kg, i.m.) and sodium thiopental (25 mg/kg, i.v.), the monkeys received a surgical operation to fix their heads painlessly in a stereotaxic frame attached to a monkey chair as previously described (Nambu *et al.*, 2000, 2002b). After the skin incision, the skull was widely exposed, and its periosteum was completely removed. Small polyether ether ketone (PEEK) screws were attached to the skull as anchors. The exposed skull and screws were completely covered with transparent acrylic resin. Two PEEK pipes were mounted in parallel over the frontal and occipital areas for head fixation. All surgical procedures were performed under aseptic conditions. All materials that were attached to the monkeys' skulls were compatible with magnetic resonance imaging (MRI). Arterial oxygen saturation and heart rate were monitored during the surgery. Depth of anaesthesia was assessed by heart rate and body movements. Anaesthetic agents were additionally administrated when necessary. Antibiotics and analgesics were administered after the surgery.

A few days after the surgery, structural MRI (3D MP-RAGE, 192 axial slices, 0.8 mm thickness, TR/TE = 2500/5.16 ms, 144 × 192 matrix size, yielding to isotropic voxels of 0.8 mm) was acquired by a 3T MRI scanner (3T Allegra; Siemens, Erlangen, Germany) with painless head fixation under anaesthesia with ketamine hydrochloride (10 mg/kg, i.m.) and xylazine hydrochloride (1 mg/kg, i.m.). Arterial oxygen saturation and heart rate were monitored during MRI scanning. Depth of anaesthesia was assessed by heart rate and body movements. The MRI scan helped to localize the STN and GPe/GPi prior to electrophysiological recording and to reconstruct recording sites histologically in the STN and GPe/GPi.

Implantation of stimulating electrodes into the cerebral cortex

After full recovery from the surgery, the skull over the central sulcus and midline was removed under anaesthesia with ketamine hydrochloride (10 mg/kg, i.m.) and xylazine hydrochloride (1 mg/kg, i.m.) with local lidocaine application, and electrophysiological mapping of the MI and SMA was performed (Fig. 1; Nambu *et al.*, 2000, 2002b). According to this mapping, pairs of bipolar intracortical stimulating electrodes (composed of 200-µm-diameter enamel-coated stainless steel wires; intertip distance, 2 mm) were chronically implanted into the following regions in the MI (at a depth of 4 mm from the dural surface) and SMA (at a depth of 5 mm from the dural surface): In *Monkey P8*, the orofacial (MIo), distal forelimb (MIfd) and proximal forelimb (MIfp), and hindlimb (MIh) regions of the MI, and the orofacial (SMAo), forelimb (SMAf) and hindlimb (SMAh) regions of the SMA (Fig. 1), in *Monkey P6*, the same regions as those in *Monkey P8* except for the

SMAo. In the analyses, MIfd and MIfp were dealt with together as the forelimb region (MIf) of the MI. These stimulating electrodes were fixed to the skull with acrylic resin, and exposed cortical areas were covered with additional acrylic resin except for two openings (10–15 mm diameter) used for accessing the STN and GPe/GPi. A rectangular plastic chamber was attached to cover two openings. Depth of anaesthesia was assessed by body movements, and ketamine hydrochloride and xylazine hydrochloride were additionally administered when necessary. Antibiotics and analgesics were administered after the above procedures.

Recording of STN and GPe/GPi neuronal activity

One week after the implantation of cortical stimulating electrodes, recording neuronal activity in the STN and GPe/GPi was started in the awake state. During the recording sessions, the monkeys were calmly seated in the monkey chair with their heads restrained.

A glass-coated Elgiloy-alloy microelectrode (1.5–2.0 MΩ at 1 kHz for STN recording, 0.8–1.2 MΩ at 1 kHz for GPe/GPi recording) was inserted vertically into the STN or obliquely (50° for *Monkey P8*, 45° for *Monkey P6* from vertical in the frontal plane) into the GPe/GPi with a hydraulic microdrive (Narishige Scientific Instruments, Tokyo, Japan). Neuronal signals in the STN and GPe/GPi were amplified (8000 times), filtered (200–2 kHz) and monitored using an oscilloscope. The unitary activity was carefully isolated, converted into digital data with a home-made time–amplitude window discriminator and then sampled at 2 kHz with a computer. Spontaneous unit activity was recorded for 50 s and confirmed as a single unit activity by checking refractory periods around 0 ms in

autocorrelograms. Cortical stimulation (300-μs duration, single pulse, 0.7-mA strength, at 0.7 Hz) was delivered via the stimulating electrodes implanted in the MI and SMA. These stimulation parameters were determined by a series of our previous studies (Nambu *et al.*, 2000, 2002b; Kita *et al.*, 2004, 2005; Tachibana *et al.*, 2008; Takara *et al.*, 2011). Neuronal responses to cortical stimulation were examined and stored on the computer with constructing peristimulus time histograms (PSTHs; bin width of 1 ms; sum of 100 times). Further, in *Monkey P8*, kinaesthetic responses of each neuron to passive movement of the following body parts were examined: the orofacial part (lip and jaw), contralateral forelimb (digit, wrist, elbow, and shoulder) and hindlimb (ankle, knee and hip). Examination of kinaesthetic response was always performed by the same experimenter. The activity was audiomonitored, and the body part whose movements evoked the strongest response was determined in each neuron.

Data analysis

For each PSTH, we calculated the mean and standard deviation (SD) of the discharge rate during the 100-ms period preceding the stimulation, and considered them as the baseline discharge rate. We then indicated the mean and mean $\pm$ 1.65 SD (corresponding to $P < 0.05$, one-tailed t-test) in each PSTH by grey solid (mean) and dashed (mean $\pm$ 1.65 SD) lines, respectively (see Fig. 2). Changes in neuronal activity in response to cortical stimulation were judged to be significant if the discharge rate during at least two consecutive bins (2 ms) exceeded the dashed lines (Nambu *et al.*, 2000; Tachibana *et al.*, 2008). The latency of each response was defined as the
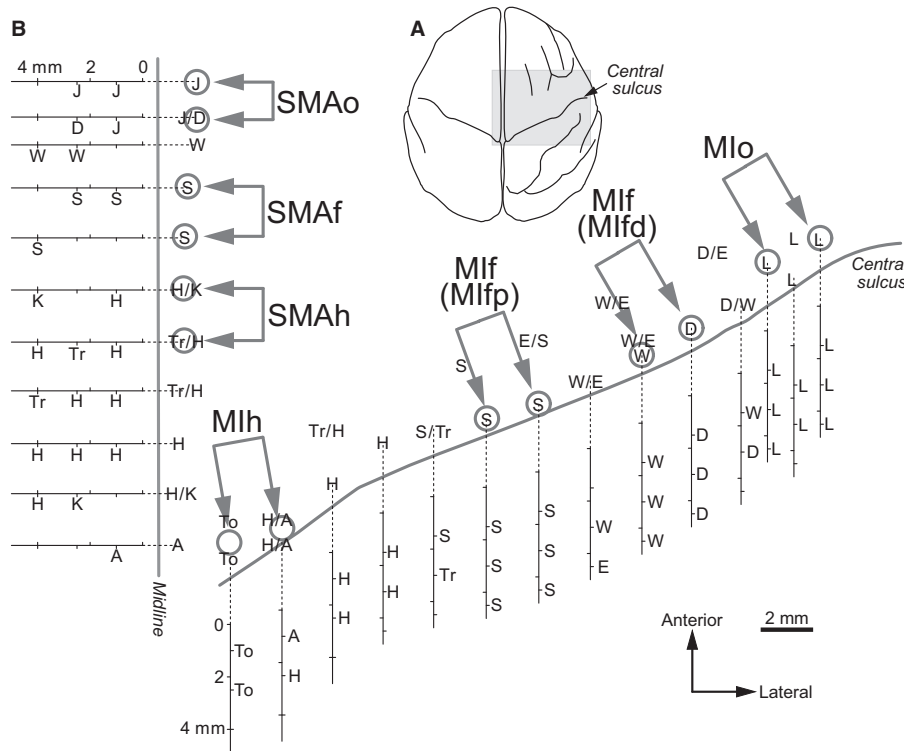
FIG. 1. Cortical mapping for the implantation of stimulating electrodes. (A) Top view of the brain of *Monkey P8*. Grey part indicates mapped area in B. (B) Mapping of supplementary motor area (SMA) and primary motor cortex (MI). Each letter indicates the somatotopic body part: A, ankle; D, digit; E, elbow; H, hip; K, knee; L, lip; J, jaw; S, shoulder; Tr, trunk; To, toe; W, wrist. Somatotopic arrangements in the mesial surface and the anterior bank of the central sulcus are also shown, along with depths from the cortical surface. Seven pairs of bipolar-stimulating electrodes were implanted into the loci indicated by small circles: the orofacial (SMAo), forelimb (SMAf) and hindlimb (SMAh) regions of the SMA and the orofacial (MIo), forelimb (MIf; distal forelimb, MIfd; proximal forelimb, MIfp) and hindlimb (MIh) regions of the MI.

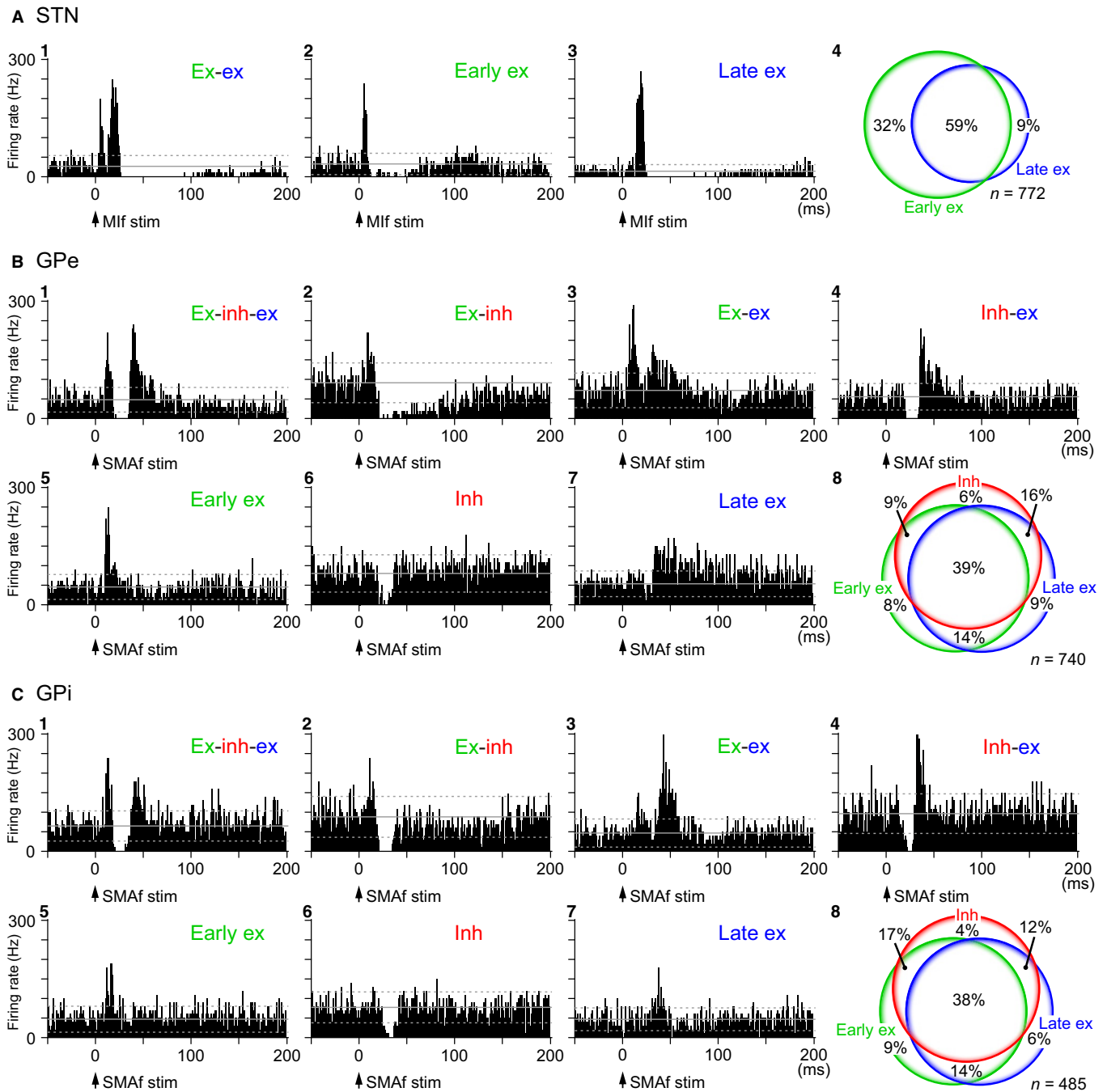FIG. 2. Neuronal responses in the subthalamic nucleus (STN), and the external (GPe) and internal (GPi) segments of the globus pallidus evoked by cortical stimulation. Typical response patterns of STN (A1–3), GPe (B1–7) and GPi (C1–7) neurons to the stimulation of the cortex are shown in peristimulus time histograms (PSTH; bin width of 1 ms; 100 stimulus trials). Cortical stimulation (duration 300 μs, single pulse, 0.7 mA) was delivered at time 0 (arrows). The mean and mean ± 1.65 SD (corresponding to $P < 0.05$, one-tailed t-test) are indicated in PSTHs by grey solid and dashed lines, respectively. The percentages of the response patterns are indicated in Venn diagrams (A4, B8, C8). An early excitation (Early ex), an inhibition (Inh) and a late excitation (Late ex) are indicated by different colours. Ex, excitation; Inh, inhibition. Ex-inh-ex indicates the response consisting of an early excitation followed by an inhibition and a late excitation.

time at which the first bin of the two consecutive bins exceeded the dashed lines. The responses were judged to end when two consecutive bins fell below the dashed lines. Because the latency of each response component was different between MI- and SMA-stimulation (Table 1), we could not set constant values as the latency thresholds for early and late excitations under all stimulus conditions. Instead, based on the observed latencies for biphasic STN responses and triphasic GPe/GPi responses (Fig. 2), we set the latency thresholds for early and late excitations as 13 ms

(MI-stimulation) and 17 ms (SMA-stimulation) in the STN and as 19 ms (MI-stimulation) and 22 ms (SMA-stimulation) in the GPe/GPi. The amplitude of each component of cortically evoked responses was defined as the number of spikes during the significant response minus that of the baseline discharge in the PSTH (i.e. the area of the response). Among cortical regions whose stimulation induced a significant response component in a neuron, the major cortical input region was defined as the cortical region whose stimulation induced the maximum amplitude of the response, and the

TABLE 1. Latency of each response component to MI- and SMA-stimulation

| Cortical stimulating site | Latency (mean ± SD, ms) | | | | | | | |
| | STN | | GPe | | | GPi | | |
	Early excitation	Late excitation	Early excitation	Inhibition	Late excitation	Early excitation	Inhibition	Late excitation
MI	6.7 ± 1.8*	17.8 ± 3.8*	9.2 ± 2.0*	16.7 ± 3.0*	28.1 ± 4.4*	10.0 ± 2.6*	19.4 ± 4.6*	28.2 ± 5.2*
MIo	7.0 ± 1.9	16.5 ± 3.1	10.3 ± 2.1	16.1 ± 2.8	27.3 ± 4.1	10.4 ± 2.0	19.0 ± 5.6	27.0 ± 5.0
MIf	6.2 ± 1.6	18.5 ± 3.7	8.9 ± 2.0	16.9 ± 3.3	27.7 ± 4.4	10.2 ± 3.0	20.1 ± 4.2	27.8 ± 4.4
MIh	7.3 ± 1.6	18.2 ± 4.6	9.2 ± 1.8	16.8 ± 2.4	29.4 ± 4.3	9.4 ± 2.3	18.5 ± 4.2	30.9 ± 5.9
SMA	9.4 ± 2.0*	25.8 ± 5.3*	12.4 ± 2.1*	22.6 ± 4.1*	34.8 ± 5.5*	13.7 ± 3.6*	25.6 ± 5.5*	38.5 ± 7.3*
SMAo	9.9 ± 1.9	32.8 ± 3.8	13.5 ± 1.9	27.8 ± 5.7	41.4 ± 5.2	14.0 ± 2.3	29.0 ± 4.8	43.8 ± 6.0
SMAf	9.2 ± 2.0	25.2 ± 4.7	12.2 ± 2.2	22.4 ± 2.9	35.3 ± 5.1	14.2 ± 4.5	25.9 ± 5.7	37.6 ± 7.1
SMAh	9.3 ± 2.0	24.6 ± 5.3	11.6 ± 1.8	20.5 ± 2.4	31.9 ± 4.4	12.0 ± 2.5	22.1 ± 3.4	34.2 ± 5.1

Numbers indicate latencies in ms (mean ± SD) of each response component (early excitation, inhibition and late excitation) in the subthalamic nucleus (STN) and the external (GPe) and internal (GPi) segments of the globus pallidus evoked by the stimulation of the orofacial, forelimb and hindlimb regions (MIo, MIf and MIh) of the primary motor cortex (MI) and the orofacial, forelimb and hindlimb regions (SMAo, SMAf and SMAh) of the supplementary motor area (SMA). *Significantly different between MI-induced and SMA-induced responses (unpaired *t*-tests, $P < 0.01$).

minor cortical regions were defined as other cortical regions. If a neuron showed a significant response to a single cortical region, the major cortical input region was defined as this cortical region.

Reconstruction of recording sites

At the end of the recording sessions, anatomically important landmarks, such as dorsal borders of the STN and GPe and border between the GPe and GPi, were marked by passing cathodal DC current (20 μA for 30 s) through the recording electrode. Then, monkeys were deeply anaesthetized with sodium pentobarbital (50 mg/kg, i.v.) and perfused transcardially with 0.1 M phosphate buffer saline (pH 7.3) followed by 10% formalin in 0.1 M phosphate buffer, 0.1 M phosphate buffer containing 10% sucrose, and finally 30% sucrose. The brains were extracted and kept in the same buffer containing 30% sucrose at 4 °C. They were cut serially into 60-μm-thick frontal sections on a freezing microtome. The sections were mounted onto gelatine-coated glass slides and stained with cresyl violet. The lesions made by current injection and traces of electrode tracks were identified. The recording sites were reconstructed according to histological data as well as MRI images (Nambu *et al.*, 2000, 2002b; Tachibana *et al.*, 2008; Takara *et al.*, 2011). The positions of the cortical stimulating electrodes were also histologically confirmed.

The recording sites were mapped on the frontal sections of the STN and GPe/GPi based on the stereotaxic coordinates during electrophysiological recording and indicated by large or small circles according to their major or minor cortical inputs, respectively. Histograms were constructed from the locations of STN and GPe/GPi neurons with major cortical inputs according to Horsley–Clark stereotaxic coordinates (Kusama & Mabuchi, 1970) along the anterior–posterior (AP), medial–lateral (ML) and dorsal–ventral (DV) axes. Their distribution according to major cortical inputs was compared (one-way ANOVA with Bonferroni *post hoc* test).

Results

Overview of cortically evoked responses of STN and GPe/GPi neurons

In this study, a total of 777 STN (463 neurons in *Monkey P8*; 314 neurons in *Monkey P6*), 503 GPe (331 in *P8*; 172 in *P6*) and 435 GPi (292 in *P8*; 143 in *P6*) neurons were recorded. Among them, we analysed 398 STN (254 in *P8*; 144 in *P6*), 343 GPe (197 in *P8*; 146 in *P6*) and 247 GPi (147 in *P8*; 100 in *P6*) neurons that

displayed significant responses to stimulation of the MI and/or SMA (Fig. 1). The spontaneous firing rates of STN, GPe and GPi neurons were 22.2 ± 11.1, 59.1 ± 26.0 and 66.2 ± 22.6 (mean ± SD) Hz, respectively.

Stimulation of the MI and/or SMA induced 772 significant responses in 398 STN neurons (several neurons responded to the stimulation of more than one cortical region). As shown in Fig. 2A, a biphasic response consisting of an early excitation followed by a late excitation was the most commonly induced (Fig. 2A1), and responses only with an early excitation (Fig. 2A2) or a late excitation (Fig. 2A3) were occasionally observed (see also Fig. 2A4). The response patterns and their distributions were similar among the cortical stimulation sites. The early and late excitations in STN neurons induced by MI-stimulation had significantly shorter latencies than those induced by SMA-stimulation (unpaired *t*-tests, $P < 0.01$; Table 1).

Similarly, stimulation of the MI and/or SMA induced 740 significant responses in 343 GPe neurons and 485 significant responses in 247 GPi neurons. As shown in Fig. 2B,C, a triphasic response consisting of an early excitation followed by an inhibition and a late excitation was the most frequently induced in both the GPe and GPi (Fig. 2B1,C1). Other types of responses lacking one or two of these components were also observed (Fig. 2B2–7,C2–7), that is, an excitation followed by an inhibition, biphasic excitations and an inhibition followed by an excitation (see also Fig. 2B8,C8). The response components in GPe and GPi neurons evoked by MI-stimulation had significantly shorter latencies than those induced by SMA-stimulation (unpaired *t*-tests, $P < 0.01$; Table 1).

Cortically evoked responses of STN neurons by MI- and SMA-stimulation

Subthalamic nucleus neurons were classified into MI-, SMA- and MI + SMA-recipient neurons based on the cortically evoked early and/or late excitations (Table 2). Around 70% of STN neurons responded exclusively either to MI-stimulation (MI-recipient neurons) or to SMA-stimulation (SMA-recipient neurons). On the other hand, the remaining 30% of STN neurons responded to both MI- and SMA-stimulation (MI + SMA-recipient neurons).

Subthalamic nucleus neurons were further classified based on the cortically evoked responses to stimulation of different somatotopic regions (Table 2). Around 80% of the MI-recipient STN neurons

responded exclusively to a single somatotopic region, and the remaining 20% of neurons responded to two adjacent somatotopic regions, such as orofacial and forelimb regions of the MI (MIo + f) and forelimb and hindlimb regions of the MI (MIf + h). SMA-recipient STN neurons tended to receive more convergent inputs from two adjacent somatotopic regions, and this tendency was more evident in MI + SMA-recipient STN neurons (Table 2).

Cortically evoked responses of GPe/GPi neurons by MI- and SMA-stimulation

External segment of the globus pallidus and GPi neurons were classified into MI-, SMA- and MI + SMA-recipient neurons based on the cortically evoked early excitation, inhibition and/or late excitation (Tables 3 and 4). Around two-thirds of GPe neurons and around

three-fourths of GPi neurons were classified as MI- or SMA-recipient neurons, and the remaining one-third of GPe neurons and one-fourth of GPi neurons as MI + SMA-recipient neurons. Around 80% of the MI-recipient GPe/GPi neurons received inputs from a single somatotopic region, and the remaining 20% of neurons received inputs from two adjacent somatotopic regions (Tables 3 and 4). SMA-recipient GPe/GPi neurons also received inputs from a single somatotopic region; however, they tended to receive more convergent inputs from two adjacent somatotopic regions. These convergent inputs were more evident in MI + SMA-recipient GPe/GPi neurons.

Locations of recorded STN neurons

Locations of STN neurons were plotted according to the cortically evoked early excitation in *Monkey P8* (Figs 3A and 4). Neurons

TABLE 2. Classification of STN neurons according to cortical inputs

	Early excitation			Late excitation		
	P8	*P6*	Total	*P8*	*P6*	Total
STN neurons	N = 249	N = 130	N = 379	N = 179	N = 144	N = 323
MI-recipient	49	68	117 (31%)	15	63	78 (24%)
Single body part	42	54	96 (82%)	15	50	65 (83%)
MIo	29	33		10	35	
MIf	10	6		2	2	
MIh	3	15		3	13	
Two adjacent parts	7	14	21 (18%)	0	13	13 (17%)
MIo + f	7	7		0	5	
MIf + h	0	7		0	8	
Other combinations	0	0	0 (0%)	0	0	0 (0%)
SMA-recipient	125	25	150 (40%)	128	31	159 (49%)
Single body part	57	20	77 (51%)	97	26	123 (77%)
SMAo	25	–		13	–	
SMAf	15	12		63	15	
SMAh	17	8		21	11	
Two adjacent parts	58	5	63 (42%)	30	5	35 (22%)
SMAo + f	38	–		15	–	
SMAf + h	20	5		15	5	
Other combinations	10	0	10 (7%)	1	0	1 (1%)
SMAo + f + h	10	–		1	–	
MI + SMA-recipient	75	37	112 (29%)	36	50	86 (27%)
Single body part	27	7	34 (30%)	27	8	35 (41%)
(MI + SMA)o	0	–		0	–	
(MI + SMA)f	27	6		27	7	
(MI + SMA)h	0	1		0	1	
Two adjacent parts	37	24	61 (55%)	8	32	40 (46%)
MIo + SMAf	1	1		0	3	
MIo + (MI + SMA)f	2	6		0	10	
SMAo + (MI + SMA)f	4	–		0	–	
MIf + SMAh	0	5		0	6	
(MI + SMA)f + MIh	0	0		0	1	
(MI + SMA)f + SMAh	16	2		2	3	
MIf + (MI + SMA)h	0	5		0	3	
(MI + SMA)f + h	0	3		1	4	
SMAf + MIh	10	1		5	1	
SMAf + (MI + SMA)h	4	1		0	1	
Other combinations	11	6	17 (15%)	1	10	11 (13%)
MIo + SMAh	1	0		0	1	
MIo + SMAf + h	2	1		1	2	
MIo + f + SMAh	0	1		0	3	
MIo + (MI + SMA)f + SMAh	3	4		0	3	
MIo + f + (MI + SMA)h	0	0		0	1	
SMAo + f + MIh	4	–		0	–	
SMAo + f + (MI + SMA)h	1	–		0	–	

Numbers of STN neurons in two monkeys (*P8* and *P6*) are shown according to responses (early and late excitations) evoked by cortical stimulation (MIo, MIf, MIh, SMAo, SMAf and SMAh).

receiving inputs from the MI and/or SMA were located in the dorsal and central STN. MI-recipient neurons were predominantly found in the posterolateral domain, while SMA-recipient neurons were mainly found in the anteromedial domain (Fig. 3A1). MI + SMA-recipient neurons were distributed in both the MI and SMA domains, especially in the transition zone between the MI and SMA domains. These distribution differences between MI-, SMA- and MI + SMA-recipient neurons were significant (Bonferroni test, $P < 0.05$; Fig. 3A2). In the lateral MI domain, MIo- and MIh-recipient neurons were located in the most lateral and the most medial parts, respectively, and MIf-recipient neurons were found in between them (Fig. 4A1). MIo-recipient neurons were found more ventrally than MIf- and MIh-recipient neurons. These distribution differences of MIo-, MIf- and MIh-recipient

neurons were significant (Bonferroni test, $P < 0.05$; Fig. 4A2). MIo + f-recipient neurons were located in the transition zone between the MIo and MIf domains. In the medial SMA domain, SMAh- and SMAf-recipient neurons were found adjacent to the MI domain, and SMAo-recipient neurons were found in the most medial part (Fig. 4B1,2). STN neurons with convergent inputs from two adjacent somatotopic regions of the SMA were found in the transition zone between two somatotopic regions of the STN. STN neurons in *Monkey P6* were located in a similar way, although their responses to SMAo-stimulation were not tested.

We also drew somatotopic maps of the STN based on the late excitation and obtained similar results to those based on the early excitation described above (Fig. 5A for MIf-stimulation). These results are expected, as the major response pattern of cortically

TABLE 3. Classification of GPe neurons according to cortical inputs

	Early excitation			Inhibition			Late excitation		
	P8	*P6*	Total	*P8*	*P6*	Total	*P8*	*P6*	Total
GPe neurons	$N = 185$	$N = 129$	$N = 314$	$N = 144$	$N = 125$	$N = 269$	$N = 144$	$N = 144$	$N = 288$
MI-recipient	59	62	121 (39%)	25	39	64 (24%)	25	40	65 (23%)
Single body part	56	50	106 (88%)	24	26	50 (78%)	25	27	52 (80%)
MIo	10	12		4	11		4	9	
MIf	15	21		4	4		1	5	
MIh	31	17		16	11		20	13	
Two adjacent parts	3	12	15 (12%)	1	13	14 (22%)	0	13	13 (20%)
MIo + f	1	3		0	10		0	11	
MIf + h	2	9		1	3		0	2	
Other combinations	0	0	0 (0%)	0	0	0 (0%)	0	0	0 (0%)
SMA-recipient	90	21	111 (35%)	85	23	108 (40%)	76	26	102 (35%)
Single body part	55	18	73 (66%)	62	22	84 (78%)	55	25	80 (78%)
SMAo	19	–		16	–		4	–	
SMAf	33	13		37	15		45	17	
SMAh	3	5		9	7		6	8	
Two adjacent parts	35	3	38 (34%)	23	1	24 (22%)	21	1	22 (22%)
SMAo + f	30	–		20	–		19	–	
SMAf + h	5	3		3	1		2	1	
Other combinations	0	0	0 (%)	0	0	0 (0%)	0	0	0 (0%)
MI + SMA-recipient	36	46	82 (26%)	34	63	97 (36%)	43	78	121 (42%)
Single body part	24	19	43 (52%)	20	10	30 (31%)	29	14	43 (36%)
(MI + SMA)o	0	–		0	–		0	–	
(MI + SMA)f	15	12		11	3		18	9	
(MI + SMA)h	9	7		9	7		11	5	
Two adjacent parts	10	25	35 (43%)	13	41	54 (56%)	13	50	63 (52%)
MIo + SMAf	1	5		0	4		3	6	
MIo + (MI + SMA)f	1	2		5	14		1	15	
SMAo + (MI + SMA)f	3	–		1	–		0	–	
MIf + SMAh	0	3		0	3		0	3	
(MI + SMA)f + MIh	0	0		0	2		2	4	
(MI + SMA)f + SMAh	0	3		0	1		0	0	
MIf + (MI + SMA)h	0	5		0	9		0	14	
(MI + SMA)f + h	0	5		0	7		1	7	
SMAf + MIh	2	1		5	0		3	0	
SMAf + (MI + SMA)h	3	1		2	1		3	1	
Other combinations	2	2	4 (5%)	1	12	13 (13%)	1	14	15 (12%)
MIo + SMAh	0	0		0	1		0	2	
MIo + SNAf + h	0	1		0	1		0	1	
MIo + f + SMAh	0	0		0	3		0	1	
MIo + (MI + SMA)f + SMAh	0	0		0	3		0	5	
MIo + f + (MI + SMA)h	0	1		0	3		0	3	
MIo + (MI + SMA)f + h	0	0		0	1		0	2	
SMAo + (MI + SMA)f + MIh	1	–		0	–		0	–	
SMAo + (MI + SMA)f + h	0	–		0	–		1	–	
SMAo + f + (MI + SMA)h	1	–		1	–		0	–	

Numbers of GPe neurons in two monkeys (*P8* and *P6*) are shown according to responses (early excitation, inhibition and late excitation) evoked by cortical stimulation (MIo, MIf, MIh, SMAo, SMAf and SMAh).

evoked responses was a biphasic response consisting of an early excitation and a late excitation (Fig. 2A), and as the categorization of STN neurons based on the early and late excitations showed similar results (Table 2).

Locations of recorded GPe/GPi neurons

Locations of GPe/GPi neurons were plotted according to the cortically evoked early excitation in *Monkey P8* (Figs 3B and 6). Neurons receiving inputs from the MI and/or SMA were located in the posterior section of the GPe/GPi. MI-recipient neurons were mainly located in the posterolateral domain, while SMA-recipient neurons were found in the more anterior and medial domain (Fig. 3B1). This distribution difference between MI- and SMA-recipient neurons was significant (Bonferroni test, $P < 0.05$; Fig. 3B2,3). MI + SMA-recipient neurons were distributed in both the MI and SMA domains, especially in the transition zone between the MI and SMA domains. In the MI domain, MIh-, MIf- and MIo-recipient neurons were arranged from the dorsal to ventral parts in the GPe/GPi (Fig. 6A1). The distribution of MIh-, MIf- and MIo-recipient neurons along the dorsal–ventral axis was significant (Bonferroni test, $P < 0.05$; Fig. 6A2,3). In the SMA domain, a

TABLE 4. Classification of GPi neurons according to cortical inputs

	Early excitation			Inhibition			Late excitation		
	P8	P6	Total	P8	P6	Total	P8	P6	Total
GPi neurons	N = 139	N = 90	N = 229	N = 119	N = 84	N = 203	N = 105	N = 96	N = 201
MI-recipient	34	59	93 (41%)	15	45	60 (30%)	16	49	65 (32%)
Single body part	31	51	82 (88%)	14	33	47 (78%)	15	33	48 (74%)
MIo	6	23		5	19		4	21	
MIf	13	15		2	2		2	2	
MIh	12	13		7	12		9	10	
Two adjacent parts	3	8	11 (12%)	1	12	13 (22%)	1	16	17 (26%)
MIo + f	2	5		1	9		1	12	
MIf + h	1	3		0	3		0	4	
Other combinations	0	0	0 (0%)	0	0	0 (0%)	0	0	0 (0%)
SMA-recipient	74	13	87 (38%)	67	15	82 (40%)	79	14	93 (46%)
Single body part	46	11	57 (66%)	50	14	64 (78%)	51	11	62 (67%)
SMAo	32	–		25	–		23	–	
SMAf	11	5		20	5		21	5	
SMAh	3	6		5	9		7	6	
Two adjacent parts	27	2	29 (33%)	16	1	17 (21%)	28	3	31 (33%)
SMAo + f	24	–		11	–		26	–	
SMAf + h	3	2		5	1		2	3	
Other combinations	1	0	1 (1%)	1	0	1 (1%)	0	0	0 (0%)
SMAo + f + h	1	–		1	–		0	–	
MI + SMA-recipient	31	18	49 (21%)	37	24	61 (30%)	10	33	43 (22%)
Single body part	16	4	20 (41%)	22	13	35 (58%)	7	7	14 (32%)
(MI + SMA)o	0	–		0	–		1	–	
(MI + SMA)f	7	3		11	10		3	3	
(MI + SMA)h	9	1		11	3		3	4	
Two adjacent parts	13	12	25 (51%)	15	9	24 (39%)	2	19	21 (49%)
MIo + SMAf	1	2		1	0		0	6	
MIo + (MI + SMA)f	2	4		2	3		0	7	
(MI + SMA)o + SMAf	1	–		1	–		0	–	
(MI + SMA)o + f	1	–		1	–		0	–	
SMAo + (MI + SMA)f	3	–		5	–		0	–	
MIf + SMAh	0	4		0	4		0	4	
(MI + SMA)f + MIh	0	0		1	0		1	0	
(MI + SMA)f + SMAh	0	0		0	1		0	1	
MIf + (MI + SMA)h	0	0		0	1		0	0	
(MI + SMA)f + h	0	1		0	0		0	1	
SMAf + MIh	2	1		1	0		1	0	
SMAf + (MI + SMA)h	3	0		3	0		0	0	
Other combinations	2	2	4 (8%)	0	2	2 (3%)	1	7	8 (19%)
MIo + SMAh	0	1		0	0		0	0	
MIo + SMAf + h	0	1		0	0		0	1	
MIo + (MI + SMA)f + SMAh	0	0		0	1		0	1	
MIo + f + SMAh	0	0		0	0		0	1	
MIo + f + (MI + SMA)h	0	0		0	0		0	2	
MIo + (MI + SMA)f + h	0	0		0	1		0	1	
MIo + SMAf + (MI + SMA)h	0	0		0	0		0	1	
SMAo + (MI + SMA)f + h	1	–		0	–		0	–	
SMAo + f + MIh	0	–		0	–		1	–	
SMAo + f + (MI + SMA)h	1	–		0	–		0	–	

Numbers of GPi neurons in two monkeys (*P8* and *P6*) are shown according to responses (early excitation, inhibition and late excitation) evoked by cortical stimulation (MIo, MIf, MIh, SMAo, SMAf and SMAh).

similar somatotopy along the dorsal–ventral axis could be observed, but was more ambiguous (Fig. 6B1–3). SMAo-recipient neurons were found in the most anterior part of the GPe/GPi. (However, see the 'Somatotopic arrangements in the GPe/GPi' in the Discussion section.) GPe/GPi neurons receiving convergent inputs from two adjacent somatotopic regions were located in the transition zone between two somatotopic regions of the GPe/GPi. These distributions of GPe/GPi neurons were found in both *Monkeys P8 and P6*, although their responses to SMAo-stimulation were not tested in *Monkey P6*.

We also drew somatotopic maps of the GPe and GPi based on the inhibition and late excitation and obtained similar results to those based on the early excitation described above (Fig. 5B for

MIf-stimulation). Again, these distributions are expected, as the major response pattern of cortically evoked responses was a triphasic response consisting an early excitation followed by an inhibition and a late excitation (Fig. 2B,C), and as the categorization of GPe/GPi neurons based on the early excitation, inhibition and late excitation showed similar results (Tables 3 and 4).

Detailed cortical inputs from the forelimb region of the MI to the STN and GPe/GPi

We further analysed the responses to stimulation of the distal (MIfd) and proximal (MIfp) forelimb regions of the MI. Among STN, GPe and GPi neurons responding to MIf- or MIf + SMA-stimulation, a
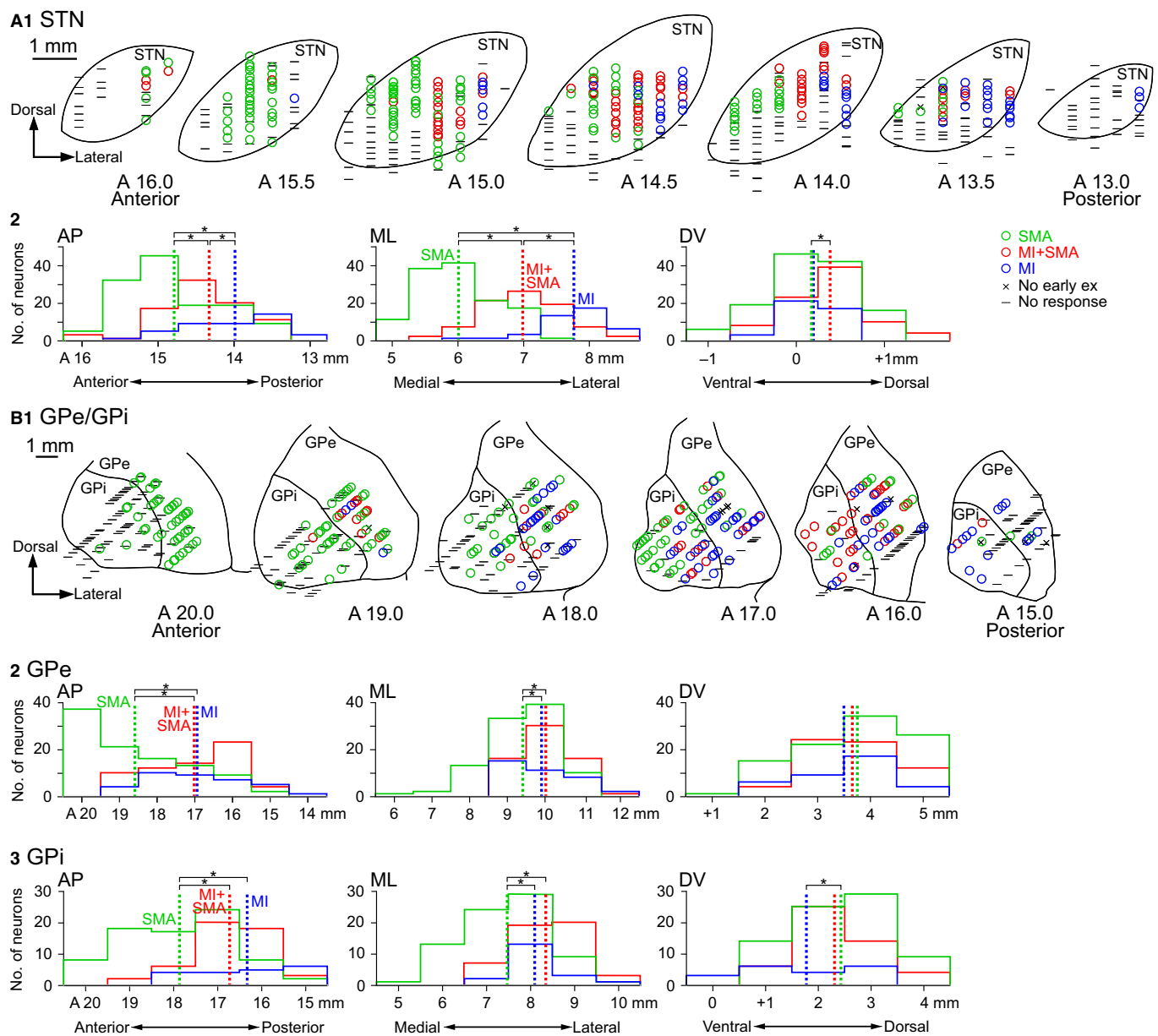

FIG. 3. Distribution of primary motor cortex (MI)- and/or supplementary motor area (SMA)-inputs in the subthalamic nucleus (STN) and GPe/GPi. Locations of STN (A1) and GPe/GPi (B1) neurons that showed an early excitation evoked by MI- and/or SMA-stimulation are indicated with different colours in *Monkey P8*. Crosses and bars represent no early excitations and no responses to MI- and/or SMA-stimulation, respectively. Sections along the anterior–posterior axis are arranged from left to right. The distance of the sections from the auditory meatus is shown in millimetres. Histograms show the locations of STN (A2), GPe (B2) and GPi (B3) neurons with MI- and/or SMA-inputs according to Horsley–Clark stereotaxic coordinates along the anterior–posterior (AP), medial–lateral (ML) and dorsal–ventral (DV) axes. Dashed vertical lines indicate means of the locations. *Significantly different (one-way ANOVA with Bonferroni *post hoc* test, $P < 0.05$).
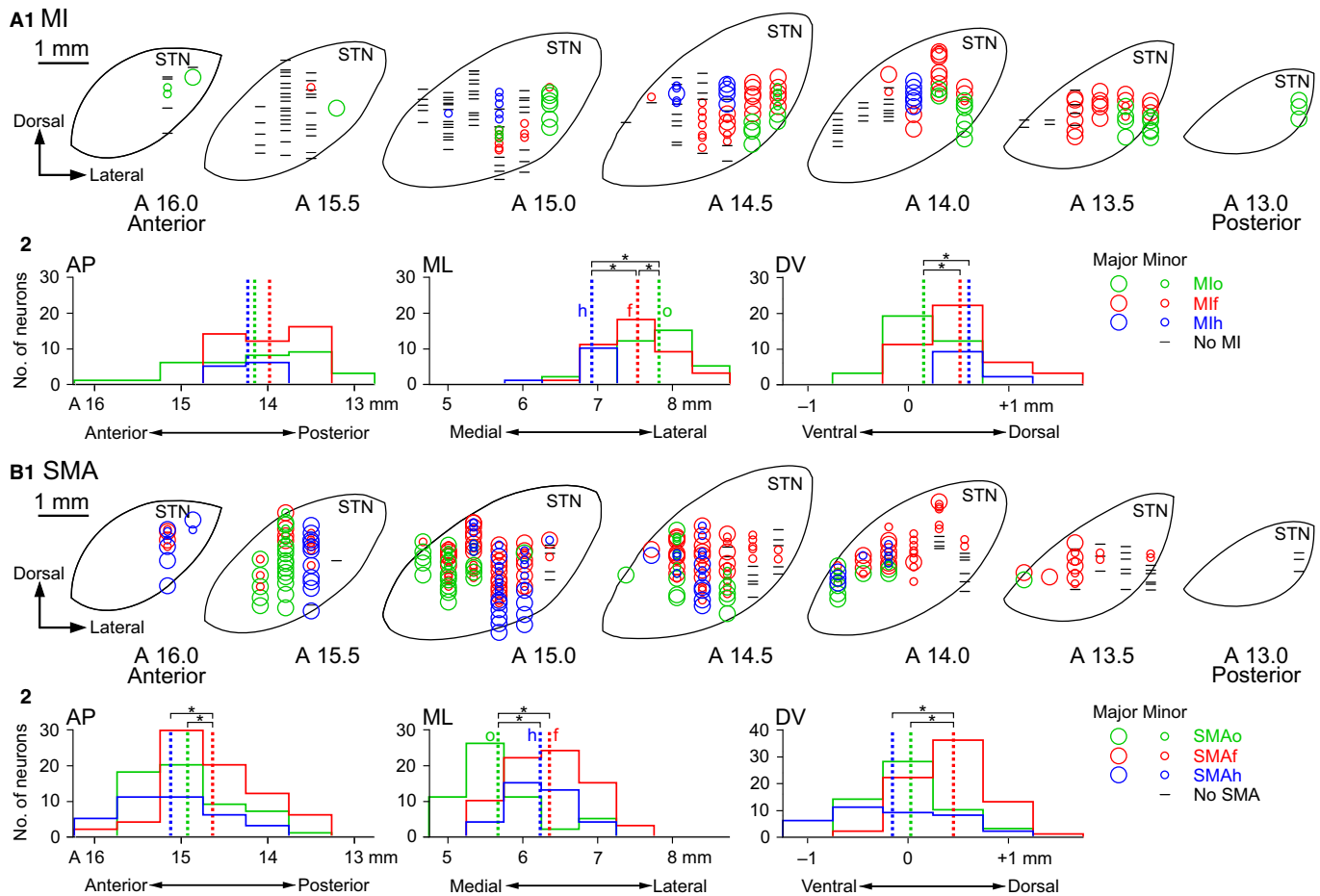
FIG. 4. Somatotopic distribution of primary motor cortex (MI)- and supplementary motor area (SMA)-inputs in the subthalamic nucleus (STN). Locations of STN neurons that showed an early excitation evoked by cortical stimulation of the somatotopic body parts in the MI (A1) and SMA (B1) in *Monkey P8* are indicated. Cortical stimulation sites, such as MIo, MIf, MIh, SMAo, SMAf and SMAh, are marked with different colours. Large circles, small circles and bars represent major cortical inputs, minor cortical inputs and no early excitations to MI- or SMA-stimulation, respectively. Histograms show the locations of STN neurons with major cortical inputs from the MI (A2) and SMA (B2) along the AP, ML and DV axes. Dashed vertical lines indicate means of the locations. *Significantly different (one-way ANOVA with Bonferroni *post hoc* test, $P < 0.05$).

certain number of them responded to stimulation of only MIfd, only MIfp or both MIfd and MIfp (MIfd + p) (Table 5). The locations of these STN and GPe/GPi neurons were plotted according to the early excitation evoked by MIfd- and MIfp-stimulation (Fig. 7). In the STN, MIfd-recipient neurons were found more laterally than MIfp-recipient neurons (Fig. 7A1, 2; Bonferroni test, $P < 0.05$), and MIfd + p-recipient neurons were located in between. In both the GPe and GPi, MIfd-recipient neurons were found more ventrally than MIfp-recipient neurons (Fig. 7B1–3; Bonferroni test, $P < 0.05$), and MIfd + p-recipient neurons were located in between.

Kinaesthetic responses of STN and GPe/GPi neurons

In *Monkey P8*, kinaesthetic responses of STN, GPe and GPi neurons exhibiting a cortically evoked early excitation were also examined (Table 6). Most of the MI-recipient and MI + SMA-recipient STN, GPe and GPi neurons showed kinaesthetic responses, typically transient increase (or occasionally decrease) of firing rates during passive joint movements and/or muscle palpation, while less of the SMA-recipient neurons did. The majority of them responded to a single body part, and the remaining neurons responded to two adjacent body parts.

Locations of neurons were plotted according to the body part whose movements evoked the strongest response in each neuron

(Fig. 8). In the STN, the neurons responding to the orofacial movements were located in the most lateral and the most medial parts, and the neurons responding to movement of the contralateral hindlimb were located in the central part (Fig. 8A). The neurons responding to movement of the contralateral forelimb were located in between. In the GPe and GPi, the neurons responding to the hindlimb, forelimb and orofacial movements were arranged from the dorsal to the ventral parts of the GPe and GPi (Fig. 8B). Such somatotopic organizations in the STN and GPe/GPi based on kinaesthetic responses agreed well with the somatotopic map based on cortically evoked responses (compare Fig. 8A with Fig. 4, and Fig. 8B with Fig. 6). In the GPe/GPi, the SMAo-recipient neurons were found widely in the anterior part while lacked sensory inputs (Figs 6B1 and 8B) (see the 'Somatotopic arrangements in the GPe/GPi' in the Discussion section).

Discussion

The present study has shown the following results: (i) stimulation of the MI and/or SMA induced a biphasic response composed of early and late excitations in the STN, and a triphasic response composed of an early excitation, an inhibition and a late excitation in the GPe and GPi (Fig. 2), as previously described (Kitai & Deniau, 1981;
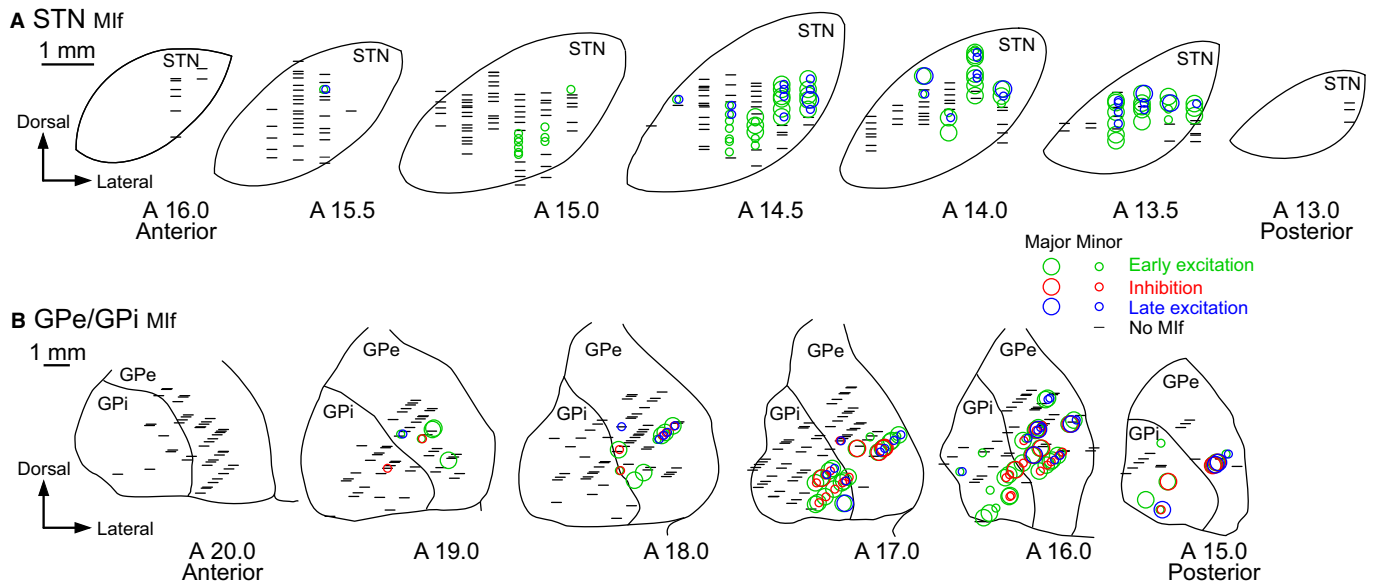
FIG. 5. Comparison of distributions of MIf-inputs based on different phases of cortically evoked responses in the subthalamic nucleus (STN) and GPe/GPi. Locations of STN (A) and GPe/GPi (B) neurons that showed responses to MIf-stimulation in *Monkey P8* are indicated. Different phases of cortically evoked responses, such as early and late excitations in STN neurons, and an early excitation, an inhibition and a late excitation in GPe/GPi neurons, are marked with different colours. Similar distributions were obtained based on different phases of evoked responses. Large circles, small circles and bars represent major cortical inputs, minor cortical inputs and no responses to MIf-stimulation, respectively.

Ryan & Clark, 1991, 1992; Kita, 1992; Fujimoto & Kita, 1993; Yoshida *et al.*, 1993; Maurice *et al.*, 1998; Nambu *et al.*, 2000, 2002a; Kita *et al.*, 2004; Tachibana *et al.*, 2008). (ii) Most of STN and GPe/GPi neurons responded exclusively to stimulation of either the MI or SMA, while one-fourth to one-third of neurons responded to stimulation of both the MI and SMA (Fig. 3, Tables 2–4). (iii) Most of MI-recipient STN and GPe/GPi neurons received inputs from a single somatotopic region. On the other hand, SMA- or MI + SMA-recipient STN and GPe/GPi neurons received inputs from a single somatotopic region or convergent inputs from two adjacent somatotopic regions (Tables 2–4). (iv) In the STN, MI-recipient neurons were predominantly found in the posterolateral domain, while SMA-recipient neurons were mainly found in the anteromedial domain (Fig. 3). MI + SMA-recipient neurons were distributed in both the MI and SMA domains, especially in the transition zone between the MI and SMA domains. (v) STN neurons responding to the hindlimb, forelimb and orofacial regions of the MI were found in the medial to lateral parts of the posterolateral STN, while neurons responding to the orofacial region of the SMA were located more medially than the others in the anteromedial STN (Fig. 4). (vi) In the GPe/GPi, MI-recipient neurons were mainly located in the posterolateral domain, while SMA-recipient neurons were found in the more anterior and medial domain (Fig. 3). MI + SMA-recipient neurons were distributed in both the MI and SMA domains, especially in the transition zone between the MI and SMA domains. (vii) GPe/GPi neurons responding to the hindlimb, forelimb and orofacial regions of the MI were found along the dorsal–ventral axis in the posterolateral GPe/GPi, and neurons responding to the corresponding regions of the SMA were similarly but less clearly distributed in more anteromedial regions (Fig. 6). (viii) Among neurons responding to the forelimb regions of the MI, those responding to the distal forelimb region were located more laterally in the STN and more ventrally in the GPe/GPi than those responding to the proximal forelimb region (Fig. 7). (ix) Most of the MI- and MI + SMA-recipient STN and GPe/GPi neurons showed

kinaesthetic responses, while less of the SMA-recipient neurons did (Table 6). The somatotopic maps based on kinaesthetic responses were similar to those based on cortically evoked responses in both the STN and GPe/GPi (Fig. 8; Compare with Figs 4 and 6). Finally, data were obtained from two female monkeys, and the present results should be further explored by extensive data from more animals, including male subjects.

Cortically evoked responses in the STN and their origins

In this study, MI- and/or SMA-stimulation commonly induced a biphasic response consisting of early and late excitations in STN neurons (Fig. 2A), as previously reported (Nambu *et al.*, 2000). The early excitation is thought to be mediated by the direct cortico-STN projection, as previously shown in rodents and primates (Kitai & Deniau, 1981; Ryan & Clark, 1992; Fujimoto & Kita, 1993; Maurice *et al.*, 1998; Nambu *et al.*, 2000). The most probable origin of the late excitation is the disinhibition of STN neurons by the cortico-striato-GPe-STN indirect pathway (Maurice *et al.*, 1998; Nambu *et al.*, 2002a), although other possibilities include rebound firings after the inhibition evoked by the cortico-STN-GPe-STN pathway (Nakanishi *et al.*, 1987; Bevan *et al.*, 2002), and a second part of a cortico-STN induced a broad excitation interrupted by a brief inhibition via the cortico-STN-GPe-STN pathway (Fujimoto & Kita, 1993). Thus, cortical information through the cortico-STN and cortico-striato-GPe-STN pathways converges on the same STN neurons, and convergence from the MI and SMA occurred to a similar extent through both projections (Table 2). The latencies of MI-evoked early and late excitations in this study were similar to those previously reported (Nambu *et al.*, 2000) and were shorter than those of SMA-evoked ones in this study (Table 1). This latency difference may be explained by the difference in conduction velocities of axons originating from the MI and SMA, as observed in the putamen (Nambu *et al.*, 2002b).
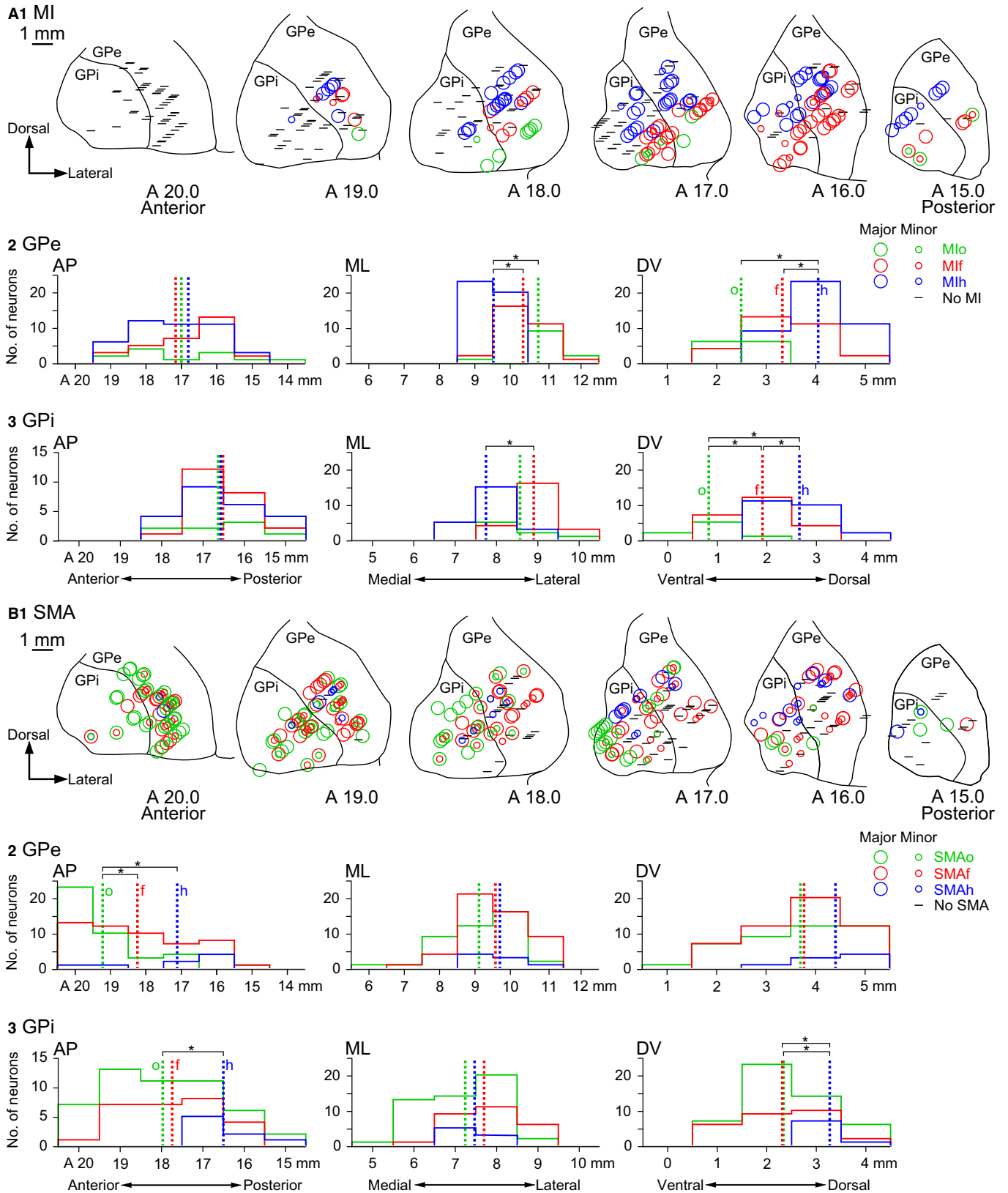
FIG. 6. Somatotopic distribution of primary motor cortex (MI)- and supplementary motor area (SMA)-inputs in the GPe/GPi. Locations of GPe/GPi neurons that showed an early excitation evoked by cortical stimulation of the somatotopic body parts in the MI (A1) and SMA (B1) in *Monkey P8* are indicated. Cortical stimulation sites, such as MIh, MIf, MIo, SMAh, SMAf and SMAo, are marked with different colours. Large circles, small circles and bars represent major cortical inputs, minor cortical inputs and no early excitations to MI- or SMA-stimulation, respectively. Histograms show the locations of GPe (A2, B2) and GPi (A3, B3) neurons with major cortical inputs from the MI (A2, 3) and SMA (B2, 3) along the AP, ML and DV axes. Dashed vertical lines indicate means of the locations. *Significantly different (one-way ANOVA with Bonferroni *post hoc* test, $P < 0.05$).

TABLE 5. Classification of STN, GPe, GPi neurons according to detailed cortical inputs from the forelimb region of the MI

	STN	GPe	GPi
MIf	37 (*P8*, 17; *P6*, 20)	51 (*P8*, 18; *P6*, 33)	39 (*P8*, 16; *P6*, 23)
MIfd	13	11	12
MIfp	12	29	15
MIfd + p	12	11	12
MIf + SMA	85 (*P8*, 53; *P6*, 32)	51 (*P8*, 31; *P6*, 20)	26 (*P8*, 12; *P6*, 14)
MIfd + SMA	21	6	9
MIfp + SMA	30	31	10
MIfd + p + SMA	34	14	7

Numbers of STN, GPe and GPi neurons in two monkeys (*P8* and *P6*) are shown according to responses (early excitation) evoked by stimulation of the distal (MIfd) and proximal (MIfp) forelimb regions of the MI and SMA.

In this study, the intensity of cortical stimulation was constantly set to 0.7 mA, which might be high. However, such cortical stimulation is considered to be confined to a limited cortical site and not to spread to other somatotopic regions or other cortical areas, because stimulation of the MI induced discrete movements of the corresponding body parts, such as thumb flexion. Moreover, activation of other cortical regions through cortico-cortical projections is less probable. If SMA-stimulation effectively activates the MI through the intercortical SMA-MI projection (Tokuno & Nambu, 2000), the distribution of MI- and MI + SMA-recipient neurons should overlap each other in the STN, contradicting the present results (Fig. 3A). Thus, MI + SMA-recipient STN neurons are considered to receive direct convergent inputs from both the MI and SMA.

Cortically evoked responses in the GPe/GPi and their origins

Cortical stimulation commonly evoked a triphasic response composed of an early excitation, an inhibition and a late excitation in GPe neurons (Fig. 2B,C), consistent with previous observations in primates and rodents (Ryan & Clark, 1991; Kita, 1992; Nambu *et al.*, 2000; Kita *et al.*, 2004). The early excitation is likely caused by the cortico-STN-GPe projections as suggested by our previous study (Nambu *et al.*, 2000). The inhibition is mediated by the cortico-striato-GPe pathway (Kita *et al.*, 2004, 2006) with possible participation of recurrent inhibition from GPe neurons themselves (Nambu *et al.*, 2000; Kita *et al.*, 2005). The late excitation is evoked mainly by the cortico-striato-GPe-STN-GPe pathway (Kita *et al.*, 2004), although other components, such as disinhibition by local axon collaterals of GPe neurons, may also contribute.

Cortical stimulation evoked a triphasic response in GPi neurons, similar to that in GPe neurons. The early excitation is likely caused by the cortico-STN-GPi hyperdirect pathway as suggested by our previous study (Nambu *et al.*, 2000). The inhibition is mainly mediated by the cortico-striato-GPi direct pathway (Nambu *et al.*, 2000; Kita *et al.*, 2006; Tachibana *et al.*, 2008), although the cortico-STN-GPe-GPi pathway may also contribute (Kita *et al.*, 2005). The late excitation is likely caused by the cortico-striato-GPe-STN-GPi indirect pathway (Nambu *et al.*, 2000; Tachibana *et al.*, 2008), although there are other possibilities, such as disinhibition via the cortico-striato-GPe-GPi pathway, rebound firings following the inhibition caused by the cortico-striato-GPi direct pathway and a second part of a long-lasting excitation interrupted by an inhibition via the cortico-striato-GPi direct pathway.

Information processing from the MI and SMA in the STN and GPe/GPi

In the present study, around 30% of STN neurons received convergent inputs from the MI and SMA based on the early excitation by the cortico-STN pathway and on the late excitation by the cortico-striato-GPe-STN pathway (Table 2). Similar convergence was reported in the cortico-putaminal projections: 20% of putaminal neurons received convergent inputs from the MI and SMA (Nambu *et al.*, 2002b). In the GPe, convergence from the MI and SMA occurred in around one-third of neurons based on the early excitation by the cortico-STN-GPe pathway, on the inhibition by the cortico-striato-GPe pathway and on the late excitation by the cortico-striato-GPe-STN-GPe pathway (Table 3). In the GPi, convergence from the MI and SMA occurred in around one-fourth of neurons based on the early excitation by the cortico-STN-GPi pathway, on the inhibition by the cortico-striato-GPi pathway and on the late excitation by the cortico-striato-GPe-STN-GPi pathway (Table 4). These results indicate that convergence of cortico-striatal or cortico-STN projections occurred to some extent, and that information through the striato-GPe/GPi, STN-GPe/GPi and GPe-STN-GPe/GPi projections is processed in a parallel fashion (Fig. 9A). Kaneda *et al.* (2002) showed that MI-, SMA- and MI + SMA-recipient neurons in the striatum project to different regions in the GPe/GPi, suggesting that striato-GPe/GPi projections are arranged in a parallel fashion.

When we look closely at the somatic information in the STN and GPe/GPi, most of the MI-recipient STN and GPe/GPi neurons received inputs from a single somatotopic region, while SMA-recipient neurons received inputs from a single somatotopic region or convergent inputs from two adjacent somatotopic regions: a considerable percentage of SMA-recipient neurons received convergent inputs, which is more evident in *Monkey P8*, likely because the neuronal response to SMAo-stimulation was also included in this subject (Tables 2–4). Moreover, MI + SMA-recipient neurons received more convergent inputs from two adjacent somatotopic regions. These data suggest that somatic information originating from the MI is processed mainly in a parallel fashion and that information from the SMA is processed in a convergent fashion, at least to some extent (Fig. 9A). They also suggest that both functional (i.e. MI and SMA) and somatic information are simultaneously integrated into MI + SMA-recipient neurons. The convergence of somatic information in the STN and GPe/GPi did not occur randomly, that is, convergent inputs came from the same or neighbouring somatotopic regions (Tables 2–4), indicating that the convergence seems to be functionally significant.

Somatotopic arrangements in the STN

MI-recipient neurons were mainly located in the posterolateral STN, whereas SMA-recipient neurons were mainly found in the anteromedial STN (Figs 3A and 4). In the MI domain, MIo-, MIf- and MIh-recipient neurons were located in this order from lateral to medial, while in the SMA domain, SMAo-recipient neurons were located more medially than SMAf- and SMAo-recipient neurons (Fig. 4). This somatotopic organization in the STN agrees with previous anatomical studies (Monakow *et al.*, 1978; Nambu *et al.*, 1996) (Fig. 9B). A previous anatomical study also showed that the MI sends minor projections to the medial SMA domain and the SMA to the lateral MI domain in a somatotopic organized manner (Nambu *et al.*, 1996), which supports the current observation that a considerable number of MI + SMA-recipient STN neurons received
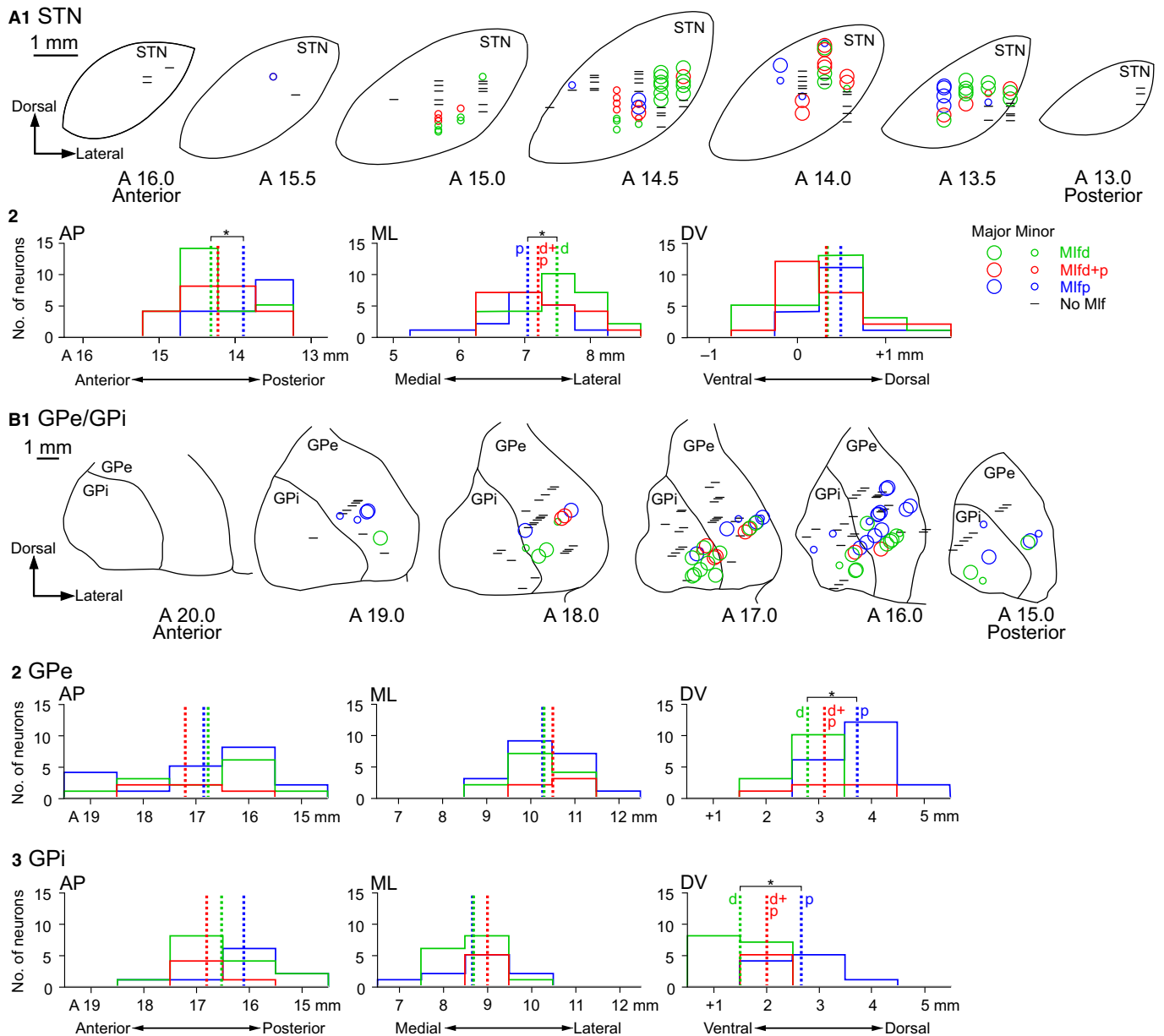
FIG. 7. Detailed somatotopic distribution of cortical inputs from the forelimb regions of the primary motor cortex (MI) in the subthalamic nucleus (STN) and GPe/GPi. Locations of STN (A1) and GPe/GPi (B1) neurons that showed an early excitation evoked by stimulation of the distal (MIfd), proximal (MIfp) or both (MIfd + p) forelimb regions of the MI in *Monkey P8* are indicated. Large circles, small circles and bars represent major cortical inputs, minor cortical inputs and no early excitations to MIf-stimulation, respectively. Histograms show the locations of STN (A2), GPe (B2) and GPi (B3) neurons with major cortical inputs along the AP, ML and DV axes. Dashed vertical lines indicate means of the locations. *Significantly different (one-way ANOVA with Bonferroni *post hoc* test, $P < 0.05$).

convergent inputs from the same somatotopic regions of the MI and SMA (Table 2).

In the present study, kinaesthetic responses of each neuron were also examined, and many neurons in both the MI and SMA domains of the STN changed their activity in relation to passive movements of the corresponding body parts (Table 6, Fig. 8A). Previous studies examining neuronal responses to active and passive movements of individual body parts revealed a somatotopic map in the STN, that is, along the medial–lateral axis of the nucleus, neurons representing the hindlimb, forelimb and orofacial regions were located (DeLong *et al.*, 1985; Wichmann *et al.*, 1994). This representation agrees well with the somatotopic organization of the MI domain in this study (Figs 4, 8A and 9B). The present study also showed

kinaesthetic responses of SMA-recipient neurons with a somatotopic arrangement, and no such movement-related activity was reported previously in the medial part of the STN. Further studies on movement-related activity of SMA-recipient STN neurons are warranted.

Somatotopic arrangements in the GPe/GPi

The ventral two-thirds of the posterior parts of the GPe/GPi is considered to be motor territories and to receive motor cortical inputs via the posterior putamen (Smith & Parent, 1986; Parent, 1990). In the present study, we examined the motor territory of the GPe/GPi and showed that the SMA domain was anterior and medial to the MI domain and that the MI + SMA-recipient neurons were found

mainly in the transition zone between the MI and SMA domains (Figs 3B and 6), supporting the findings of previous studies (Hedreen & DeLong, 1991; Hazrati & Parent, 1992; Yoshida *et al.*, 1993; Kaneda *et al.*, 2002). In the MI domain, MIh-, MIf- and MIo-recipient neurons were found along the dorsal–ventral axis (Fig. 6). In the SMA domain, a similar somatotopy along the dorsal–ventral axis could be observed, but was not as distinct as that in the MI domain (Fig. 9B). The SMAo-recipient neurons were found widely in the anterior part while lacked sensory inputs (Figs 6B and 8B). This was probably because stimulation of the SMAo, which was a small area, might spread to the pre-SMA and excite pre-SMA-recipient GPe/GPi neurons. Previous transsynaptic anterograde and retrograde labelling studies by injecting herpes simplex virus into the MI showed similar somatotopic maps to those in our current study (Hoover & Strick, 1993, 1999; Strick *et al.*, 1995; Akkal *et al.*, 2007).

In the present study, many neurons in both the MI and SMA domains of the GPe/GPi changed their activity in relation to passive movements of the corresponding body parts (Table 6, Fig. 8B). Previous studies showed that neurons responding to active and passive movements of hindlimb, forelimb and orofacial parts were found in

TABLE 6. Numbers of STN, GPe and GPi neurons showing kinaesthetic responses according to cortical inputs

	STN (%)	GPe (%)	GPi (%)
All	199/249 (80)	154/185 (83)	105/139 (76)
MI-recipient	46/49 (94)	53/59 (90)	31/34 (91)
Single body part	36 (78)	33 (62)	26 (84)
Two adjacent parts	10 (22)	20 (38)	5 (16)
SMA-recipient	85*/125 (68)	67/90 (74)	49/74 (67)
Single body part	46 (54)	44 (66)	28 (57)
Two adjacent parts	38 (45)	23 (34)	21 (43)
MI + SMA-recipient	68/75 (91)	34/36 (94)	25/31 (81)
Single body part	43 (63)	20 (59)	16 (64)
Two adjacent parts	25 (37)	14 (41)	9 (36)

Numbers and percentage of STN, GPe and GPi neurons with kinaesthetic responses are shown according to responses (early excitation) evoked by MI- and SMA-stimulation in *Monkey P8*. *Includes one STN neuron showing kinaesthetic response to all three body parts.

this order along the dorsal–ventral axis in the posterior GPe/GPi (DeLong, 1971; Georgopoulos *et al.*, 1983; DeLong *et al.*, 1985; Hamada *et al.*, 1990), which corresponds well to the current somatotopic maps in the MI domain and, to some extent, the SMA domain (Figs 6, 8B and 9B). Further studies on the activity difference between SMA- and MI-recipient GPe/GPi neurons may be warranted.

Detailed somatotopy in the STN and GPe/GPi

We further mapped responses of STN and GPe/GPi neurons to MIfd- and MIfp-stimulation. STN neurons responding to MIfd-stimulation were located more laterally than those to MIfp-stimulation in the STN (Fig. 7A). GPe/GPi neurons responding to MIfd-stimulation were located more ventrally than those to MIfp-stimulation in the GPe/GPi (Fig. 7B). These observations suggest that in the forelimb regions, distal regions are located more laterally in the STN and more ventrally in the GPe/GPi than proximal regions (Fig. 9B). To our best knowledge, this is the first report demonstrating detailed somatotopic arrangements in the STN and GPe/GPi. These arrangements are expected when we consider that the somatotopic map representing the orofacial, distal forelimb, proximal forelimb, trunk and hindlimb in the MI is transferred to the STN and to the GPe/GPi with their topography maintained along the information flow through the cortico-basal ganglia pathway. Similar distribution of STN and GPe/GPi neurons can be observed in kinaesthetic response maps to passive manipulations of digits and wrist against elbow and shoulder (Fig. 8).

Clinical significance

The GPi and STN are the target nuclei of stereotactic surgery, including deep brain stimulation for the treatment of movement disorders, such as Parkinson's disease, dyskinesia and dystonia. Similar somatotopic arrangements to the ones revealed in the present study were also observed in the human STN and GPi during stereotactic surgery (Vitek *et al.*, 1998; Rodriguez-Oroz *et al.*, 2001; Theodosopoulos *et al.*, 2003; Romanelli *et al.*, 2004; Baker *et al.*, 2010). The target areas of stereotactic surgery are motor territories
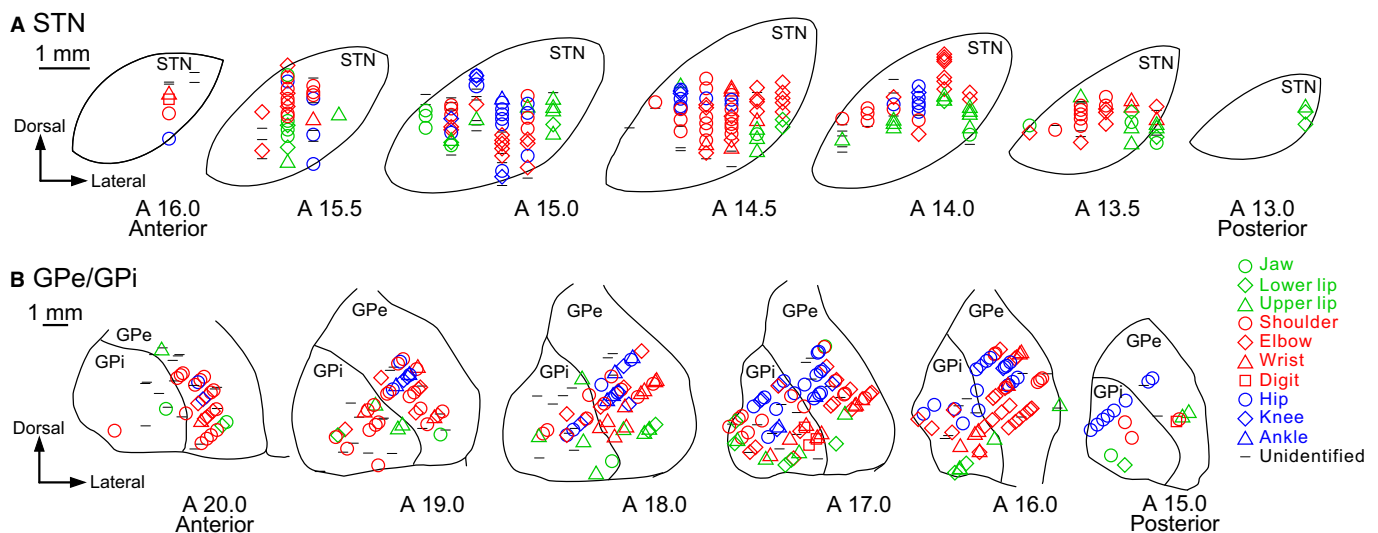

FIG. 8. Somatotopic distribution of kinaesthetic responses in the subthalamic nucleus (STN) and GPe/GPi. Locations of STN (A) and GPe/GPi (B) neurons that showed kinaesthetic responses to passive movements of body parts in *Monkey P8* are indicated. Each symbol with different colour represents the body part whose movement evoked the largest responses, and a bar indicates no response to any movements examined.
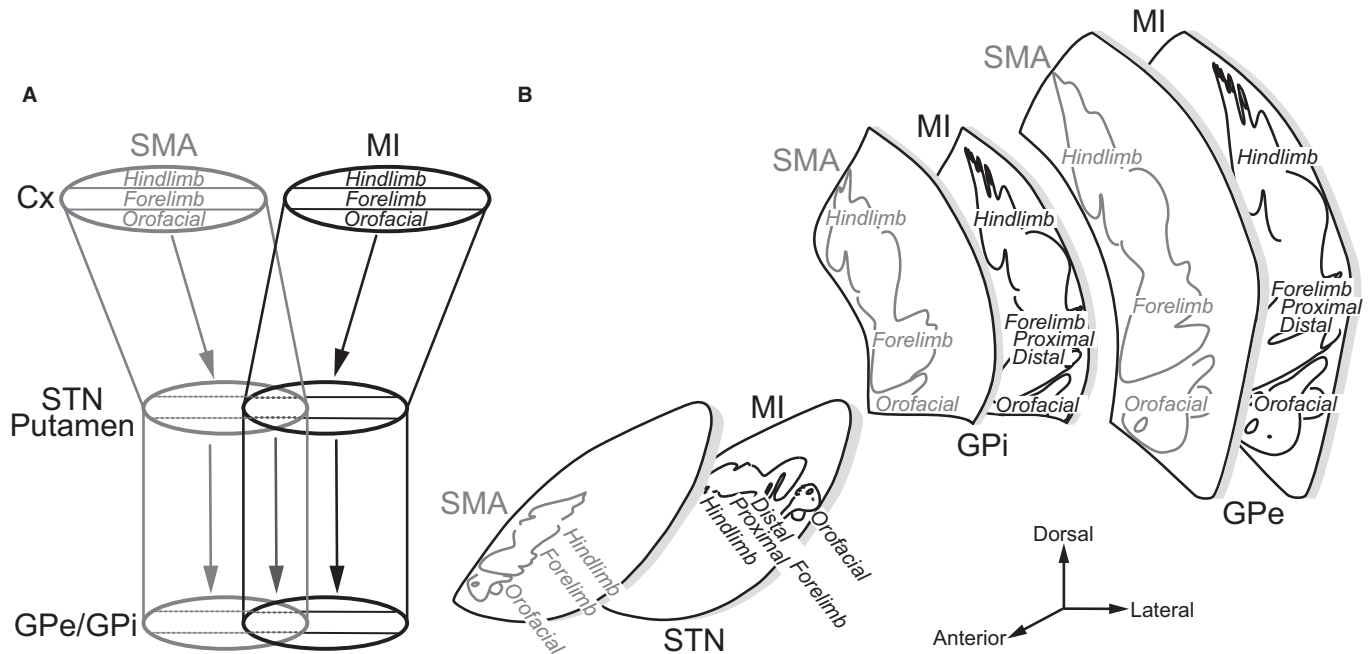
FIG. 9. Neuronal information processing in the cortico-basal ganglia projections and somatotopy in the STN and GPe/GPi. (A) Projections from the SMA and MI to the STN and putamen converge to some extent (upper), whereas projections from the STN and putamen to the GPe/GPi are parallel (lower). The information from the MI to the GPe/GPi through the STN or putamen retains its somatotopic representation, while that from the SMA is less clearly represented. (B) Somatotopic representations of the STN and GPe/GPi based on the present and previous (Nambu *et al.*, 1996) studies. In the STN, the posterolateral part receives somatotopic inputs from the MI and the anteromedial part from the SMA. In the GPe/GPi, the posterolateral parts belong to the MI domain, and the SMA domain is located anterior and medial to the MI domain.

of the STN and GPi, and microelectrode recordings and kinaesthetic responses are used to localize the targets. Moreover, pallidotomy in one somatotopic region improves symptoms in the corresponding body part, while DBS activates the stimulated structures, including their outputs and inputs, and may not have the same discrete effect (Deogaonkar & Vitek, 2009). Therefore, identification of motor territories and somatotopy in the STN and GPe/GPi is crucial for stereotactic surgery. Detailed analysis and deep understanding of somatotopic maps in the STN and GPe/GPi in non-human primates, such as those performed in the current study, should help to precisely localize the target structure of stereotactic surgery in human patients.

Acknowledgements

Conflict of interest

None declared.

Author contributions

HI performed experiments, analysed data and wrote the first draft of the manuscript. YT helped to perform the experiments and reviewed and gave critiques of the manuscript. YU and NS reviewed and gave critiques of the manuscript. AN devised the whole experiment, supervised the whole process and wrote the final version of the manuscript.

Data accessibility

The data presented in the current manuscript can be available upon request to the corresponding author (nambu@nips.ac.jp).

Abbreviations

AP, anterior–posterior axis; DV, dorsal–ventral axis; GPe, external segment of the globus pallidus; GPi, internal segment of the globus pallidus; MIfd, distal forelimb region of the primary motor cortex; MIf, forelimb region of the primary motor cortex; MIfp, proximal forelimb region of the primary motor cortex; MIh, hindlimb region of the primary motor cortex; MIo, orofacial region of the primary motor cortex; MI, primary motor cortex; ML, medial–lateral axis; MRI, magnetic resonance imaging; PEEK, polyether ether ketone; PM, premotor cortex; Pre-SMA, pre-supplementary motor area; PSTH, peristimulus time histograms; SD, standard deviation; SMAf, forelimb region of the supplementary motor area; SMAh, hindlimb region of the supplementary motor area; SMAo, orofacial region of the supplementary motor area; SMA, supplementary motor area ; SNr, substantia nigra pars reticulata; STN, subthalamic nucleus.

References

Akkal, D., Dum, R.P. & Strick, P.L. (2007) Supplementary motor area and presupplementary motor area: targets of basal ganglia and cerebellar output. *J. Neurosci.*, **27**, 10659–10673.

Albin, R.L., Young, A.B. & Penney, J.B. (1989) The functional anatomy of basal ganglia disorders. *Trends Neurosci.*, **12**, 366–375.

Alexander, G.E. & Crutcher, M.D. (1990a) Functional architecture of basal ganglia circuits: neural substrates of parallel processing. *Trends Neurosci.*, **13**, 266–271.

Alexander, G.E. & Crutcher, M.D. (1990b) Preparation for movement: neural representations of intended direction in three motor areas of the monkey. *J. Neurophysiol.*, **64**, 133–150.

Alexander, G.E. & DeLong, M.R. (1985) Microstimulation of the primate neostriatum. II. Somatotopic organization of striatal microexcitable zones and their relation to neuronal response properties. *J. Neurophysiol.*, **53**, 1417–1430.

Alexander, G.E., DeLong, M.R. & Strick, P.L. (1986) Parallel organization of functionally segregated circuits linking basal ganglia and cortex. *Annu. Rev. Neurosci.*, **9**, 357–381.

Baker, K.B., Lee, J.Y., Mavinkurve, G., Russo, G.S., Walter, B., DeLong, M.R., Bakay, R.A. & Vitek, J.L. (2010) Somatotopic organization in the internal segment of the globus pallidus in Parkinson's disease. *Exp. Neurol.*, **222**, 219–225.

Bevan, M.D., Magill, P.J., Hallworth, N.E., Bolam, J.P. & Wilson, C.J. (2002) Regulation of the timing and pattern of action potential generation in rat subthalamic neurons in vitro by GABA-A IPSPs. *J. Neurophysiol.*, **87**, 1348–1362.

DeLong, M.R. (1971) Activity of pallidal neurons during movement. *J. Neurophysiol.*, **34**, 414–427.

DeLong, M.R., Crutcher, M.D. & Georgopoulos, A.P. (1985) Primate globus pallidus and subthalamic nucleus: functional organization. *J. Neurophysiol.*, **53**, 530–543.

Deogaonkar, M. & Vitek, J.L. (2009). Globus pallidus stimulation for Parkinson'd disease. In Lozano, A.M., Gildenberg, P.L. & Tasker, R.R. (Eds), *Textbook of Stereotactic and Functional Neurosurgery*. Springer, Berlin, pp. 1577–1602.

Flaherty, A.W. & Graybiel, A.M. (1993) Two input systems for body representations in primate striatal matrix: experimental evidence in squirrel monkey. *J. Neurosci.*, **13**, 1120–1137.

Fujimoto, K. & Kita, H. (1993) Response characteristics of subthalamic neurons to the stimulation of the sensorimotor cortex in the rat. *Brain Res.*, **609**, 185–192.

Georgopoulos, A.P., DeLong, M.R. & Crutcher, M.D. (1983) Relations between parameters of step-tracking movements and single cell discharge in the globus pallidus and subthalamic nucleus of the behaving monkey. *J. Neurosci.*, **3**, 1586–1598.

Gross, R.E., Krack, P., Rodriguez-Oroz, M.C., Rezai, A.R. & Benabid, A.L. (2006) Electrophysiological mapping for the implantation of deep brain stimulators for Parkinson's disease and tremor. *Movement Disord.*, **21** (Suppl 14), S259–S283.

Haber, S.N., Kim, K.S., Mailly, P. & Calzavara, R. (2006) Reward-related cortical inputs define a large striatal region in primates that interface with associative cortical connections, providing a substrate for incentive-based learning. *J. Neurosci.*, **26**, 8368–8376.

Hamada, I., Delong, M.R. & Mano, N. (1990) Activity of identified wrist-related pallidal neurons during step and ramp wrist movements in the monkey. *J. Neurophysiol.*, **64**, 1892–1906.

Haynes, W.I. & Haber, S.N. (2013) The organization of prefrontal-subthalamic inputs in primates provides an anatomical substrate for both functional specificity and integration: implications for Basal Ganglia models and deep brain stimulation. *J. Neurosci.*, **33**, 4804–4814.

Hazrati, L.N. & Parent, A. (1992) The striatopallidal projection displays a high degree of anatomical specificity in the primate. *Brain Res.*, **592**, 213–227.

Hedreen, J.C. & DeLong, M.R. (1991) Organization of striatopallidal, striatonigral, and nigrostriatal projections in the macaque. *J. Comp. Neurol.*, **304**, 569–595.

Hoover, J.E. & Strick, P.L. (1993) Multiple output channels in the basal ganglia. *Science*, **259**, 819–821.

Hoover, J.E. & Strick, P.L. (1999) The organization of cerebellar and basal ganglia outputs to primary motor cortex as revealed by retrograde transneuronal transport of herpes simplex virus type 1. *J. Neurosci.*, **19**, 1446–1463.

Kaneda, K., Nambu, A., Tokuno, H. & Takada, M. (2002) Differential processing of motor information via striatopallidal and striatonigral projections. *J. Neurophysiol.*, **88**, 1420–1432.

Kita, H. (1992) Responses of globus pallidus neurons to cortical stimulation: intracellular study in the rat. *Brain Res.*, **589**, 84–90.

Kita, H., Chang, H.T. & Kitai, S.T. (1983) The morphology of intracellularly labeled rat subthalamic neurons: a light microscopic analysis. *J. Comp. Neurol.*, **215**, 245–257.

Kita, H., Nambu, A., Kaneda, Y., Tachibana, Y. & Takada, M. (2004) Role of ionotropic glutamatergic and GABAergic inputs on the firing activity of neurons in the external pallidum in awake monkeys. *J. Neurophysiol.*, **92**, 3069–3084.

Kita, H., Tachibana, Y., Nambu, A. & Chiken, S. (2005) Balance of monosynaptic excitatory and disynaptic inhibitory responses of the globus pallidus induced after stimulation of the subthalamic nucleus in the monkey. *J. Neurosci.*, **25**, 8611–8619.

Kita, H., Chiken, S., Tachibana, Y. & Nambu, A. (2006) Origins of GABAA and GABAB receptor-mediated responses of globus pallidus after stimulation of the putamen in the monkey. *J. Neurosci.*, **26**, 6554–6562.

Kitai, S.T. & Deniau, J.M. (1981) Cortical inputs to the subthalamus: intracellular analysis. *Brain Res.*, **214**, 411–415.

Künzle, H. (1975) Bilateral projections from precentral motor cortex to the putamen and other parts of the basal ganglia. An autoradiographic study in *Macaca fascicularis*. *Brain Res.*, **88**, 195–209.

Kusama, T. & Mabuchi, M. (1970). *Stereotaxic Atlas of the Brain of* Macaca fuscata. University of Tokyo Press, Tokyo.

Maiti, T.K., Konar, S., Bir, S., Kalakoti, P. & Nanda, A. (2016) Intra-operative micro-electrode recording in functional neurosurgery: past, present, future. *J. Clin. Neurosci.*, **32**, 166–172.

Maurice, N., Deniau, J.M., Glowinski, J. & Thierry, A.M. (1998) Relationships between the prefrontal cortex and the basal ganglia in the rat: physiology of the corticosubthalamic circuits. *J. Neurosci.*, **18**, 9539–9546.

Monakow, K.H., Akert, K. & Künzle, H. (1978) Projections of the precentral motor cortex and other cortical areas of the frontal lobe to the subthalamic nucleus in the monkey. *Exp. Brain Res.*, **33**, 395–403.

Nakanishi, H., Kita, H. & Kitai, S.T. (1987) Electrical membrane properties of rat subthalamic neurons in an in vitro slice preparation. *Brain Res.*, **437**, 35–44.

Nambu, A. (2011) Somatotopic organization of the primate basal ganglia. *Front. Neuroanat.*, **5**, 26.

Nambu, A., Yoshida, S. & Jinnai, K. (1990) Discharge patterns of pallidal neurons with input from various cortical areas during movement in the monkey. *Brain Res.*, **519**, 183–191.

Nambu, A., Takada, M., Inase, M. & Tokuno, H. (1996) Dual somatotopical representations in the primate subthalamic nucleus: evidence for ordered but reversed body-map transformations from the primary motor cortex and the supplementary motor area. *J. Neurosci.*, **16**, 2671–2683.

Nambu, A., Tokuno, H., Hamada, I., Kita, H., Imanishi, M., Akazawa, T., Ikeuchi, Y. & Hasagawa, N. (2000) Excitatory cortical inputs to pallidal neurons via the subthalamic nucleus in the monkey. *J. Neurophysiol.*, **84**, 289–300.

Nambu, A., Tokuno, H. & Takada, M. (2002a) Functional significance of the cortico-subthalamo-pallidal 'hyperdirect' pathway. *Neurosci. Res.*, **43**, 111–117.

Nambu, A., Kita, H., Akazawa, T., Imanishi, M. & Takada, M. (2002b) Organization of corticostriatal inputs in monkey putamen. *J. Neurophysiol.*, **88**, 1830–1842.

Obeso, J.A., Rodriguez-Oroz, M.C., Benitez-Temino, B., Blesa, F.J., Guridi, J., Marin, C. & Rodriguez, M. (2008) Functional organization of the basal ganglia: therapeutic implications for Parkinson's disease. *Movement Disord.*, **23**(Suppl 3), S548–S559.

Parent, A. (1990) Extrinsic connections of the basal ganglia. *Trends Neurosci.*, **13**, 254–258.

Percheron, G. & Filion, M. (1991) Parallel processing in the basal ganglia: up to a point. *Trends Neurosci.*, **14**, 55–59.

Percheron, G., Francois, C., Yelnik, J., Fenelon, G. & Talbi, B. (1994). The basal ganglia related system of primates: definition, description and information analysis. In Percheron, G., McKenzie, J.S. & Feger, J. (Eds), *The Basal Ganglia IV: New Ideas and Data on Structure and Function*. Plenum Press, New York, pp. 3–20.

Rodriguez-Oroz, M.C., Rodriguez, M., Guridi, J., Mewes, K., Chockkman, V., Vitek, J., DeLong, M.R. & Obeso, J.A. (2001) The subthalamic nucleus in Parkinson's disease: somatotopic organization and physiological characteristics. *Brain*, **124**, 1777–1790.

Romanelli, P., Heit, G., Hill, B.C., Kraus, A., Hastie, T. & Bronte-Stewart, H.M. (2004) Microelectrode recording revealing a somatotopic body map in the subthalamic nucleus in humans with Parkinson disease. *J. Neurosurg.*, **100**, 611–618.

Ryan, L.J. & Clark, K.B. (1991) The role of the subthalamic nucleus in the response of globus pallidus neurons to stimulation of the prelimbic and agranular frontal cortices in rats. *Exp. Brain Res.*, **86**, 641–651.

Ryan, L.J. & Clark, K.B. (1992) Alteration of neural responses in the subthalamic nucleus following globus pallidus and neostriatal lesions in rats. *Brain Res. Bull.*, **29**, 319–327.

Sato, F., Parent, M., Levesque, M. & Parent, A. (2000) Axonal branching pattern of neurons of the subthalamic nucleus in primates. *J. Comp. Neurol.*, **424**, 142–152.

Smith, T. & Parent, A. (1986) Differential connections of caudate nucleus and putamen in the squirrel monkey (*Saimiri sciureus*). *Neuroscience*, **18**, 347–371.

Strick, P.L., Dum, R.P. & Picard, N. (1995). Macro-organization of circuits connecting the basal ganglia with the cortical motor areas. In Houck, J.C., Davis, J.L. & Beiser, D.G. (Eds), *Models of Information Processing in the Basal Ganglia*. MIT Press, Cambridge, pp. 117–130.

Tachibana, Y., Kita, H., Chiken, S., Takada, M. & Nambu, A. (2008) Motor cortical control of internal pallidal activity through glutamatergic and GABAergic inputs in awake monkeys. *Eur. J. Neurosci.*, **27**, 238–253.

Takada, M., Tokuno, H., Nambu, A. & Inase, M. (1998) Corticostriatal projections from the somatic motor areas of the frontal cortex in the macaque monkey: segregation versus overlap of input zones from the primary motor cortex, the supplementary motor area, and the premotor cortex. *Exp. Brain Res.*, **120**, 114–128.

Takara, S., Hatanaka, N., Takada, M. & Nambu, A. (2011) Differential activity patterns of putaminal neurons with inputs from the primary motor cortex and supplementary motor area in behaving monkeys. *J. Neurophysiol.*, **106**, 1203–1217.

Theodosopoulos, P.V., Marks, W.J. Jr, Christine, C. & Starr, P.A. (2003) Locations of movement-related cells in the human subthalamic nucleus in Parkinson's disease. *Movement Disord.*, **18**, 791–798.

Tokuno, H. & Nambu, A. (2000) Organization of nonprimary motor cortical inputs on pyramidal and nonpyramidal tract neurons of primary motor cortex: an electrophysiological study in the macaque monkey. *Cereb. Cortex*, **10**, 58–68.

Vitek, J.L., Bakay, R.A., Hashimoto, T., Kaneoke, Y., Mewes, K., Zhang, J.Y., Rye, D., Starr, P. *et al.* (1998) Microelectrode-guided pallidotomy: technical approach and its application in medically intractable Parkinson's disease. *J. Neurosurg.*, **88**, 1027–1043.

Vitek, J.L., Chockkan, V., Zhang, J.Y., Kaneoke, Y., Evatt, M., DeLong, M.R., Triche, S., Mewes, K. *et al.* (1999) Neuronal activity in the basal ganglia in patients with generalized dystonia and hemiballismus. *Ann. Neurol.*, **46**, 22–35.

Wichmann, T., Bergman, H. & DeLong, M.R. (1994) The primate subthalamic nucleus. I. Functional properties in intact animals. *J. Neurophysiol.*, **72**, 494–506.

Yelnik, J. & Percheron, G. (1979) Subthalamic neurons in primates: a quantitative and comparative analysis. *Neuroscience*, **4**, 1717–1743.

Yoshida, S., Nambu, A. & Jinnai, K. (1993) The distribution of the globus pallidus neurons with input from various cortical areas in the monkeys. *Brain Res.*, **611**, 170–174.